2'-5'-oligoadenylate synthetase1 (OAS1): Molecular, structural, integrative Bioinformatics and functional analysis in the endometrium of goat (Capra hircus)

Asit Jain[1], Tripti Jain[1], Girish Kumar Mishra[1], Khushboo Chandrakar[2], Kishore Mukherjee[2], and Sita Prasad Tiwari[1]

[1]Nanaji Deshmukh Veterinary Science University
[2]Chhattisgarh Kamdhenu Vishwavidyalaya

July 12, 2022

Abstract

An interferon-inducible gene, 2'-5'-oligoadenylate synthetase-1 (OAS1), plays an essential role in uterine receptivity and conceptus development by controlling cell growth and differentiation in addition to its anti-viral activities. However, the specific part of OAS1 is not yet documented in the goat. Therefore, in the present study, the coding sequence (CDS) of the OAS1 gene was amplified, sequenced and characterized through various Bioinformatics tools. Its temporal expression profile was also examined in the endometrium of caprine (cp) for the first time. A fragment of the cpOAS1 gene, 890 bp in length, was amplified from complementary DNA (cDNA). Nucleotide and deduced amino acid sequences revealed 99.6 to 80.4 % and 99.3 to 72.3 % identities with that of ruminants and non-ruminants, respectively. A constructed phylogenetic tree revealed that sheep and goats belong to the same clade but differ from large ruminants. Besides the Physico-chemical characteristics, its localization, various posttranslational modifications, immunogenic sites, possible domains, various motifs, and interactions with other probable proteins were predicted. In addition to the secondary structure, the three-dimensional structure was predicted using homology modelling servers and a refined model, generated by the Swiss model was the best one as based on stereochemistry validated with different programs. Further, relative expression of cpOAS1 mRNA and protein was determined by quantitative real-time PCR (qPCR) and western blot, respectively, in the endometrium of pregnant and cyclic does. Caprine OAS1 protein (42/46kDa) was detected in the endometrium of pregnant and cyclic does. Both cpOAS1 mRNA and protein were expressed maximally ($P<0.05$) in the endometrium during pregnancy as compared to cyclic does. It is concluded that the cpOAS1 sequence is conserved and integrative Bioinformatics analysis provides a sound foundation for further structural and functional characterization of cpOAS1 protein in the establishment of pregnancy in goats.

Title page

Title

2'-5'-oligoadenylate synthetase1 (OAS1): Molecular, structural, integrative Bioinformatics and functional analysis in the endometrium of goat (*Capra hircus*)

Authors

Asit Jain[1]*, Tripti Jain[1], Girish Kumar Mishra[1], Khushboo Chandrakar[2], Kishore Mukherjee, Sita Prasad Tiwari[1]

Location

Molecular Genetics Laboratory, Department of Animal Genetics and Breeding, College of Veterinary Science and Animal Husbandry, Dau Shri Vasudev Chandrakar Kamdhenu Vishwavidyalaya (DSVCKV), Anjora,

Durg, Chhattisgarh, India

Author Description

[1]Currently, Nanaji Deshmukh Veterinary Science University (NDVSU), Jabalpur, Madhya Pradesh, India[2]

[2]Currently, Veterinary Assistant Surgeon, Mahasamund, Chhattisgarh, India

*Corresponding author

Corresponding Author's Details and current postal address:

Dr. Asit Jain, Associate Professor, Ph. D., Department of Animal Genetics and Breeding, College of Veterinary Science and Animal Husbandry, NDVSU, Jabalpur-482001, Madhya Pradesh, India

Telephone: +91 7587815942

E-Mail: vetasit@gmail.com

ORCID: https://orcid.org/0000-0002-1888-0507

Running Head: Structural and functional analysis of OAS1 protein in the endometrium of *Capra hircus*

2'-5'-oligoadenylate synthetase1 (OAS1): Molecular, structural, integrative Bioinformatics and functional analysis in the endometrium of goat (*Capra hircus*)

Asit Jain[1]*, Tripti Jain[1], Girish Kumar Mishra[1], Khushboo Chandrakar[2], Krishna Kishore Mukherjee, Sita Prasad Tiwari[1]

Molecular Genetics Laboratory, Department of Animal Genetics and Breeding, College of Veterinary Science and Animal Husbandry, DSVCKV, Anjora, Durg, Chhattisgarh, India

[1]Currently, Nanaji Deshmukh Veterinary Science University, Jabalpur, Madhya Pradesh, India

[2]Currently, Veterinary Assistant Surgeon, Mahasamund, Chhattisgarh, India

*Corresponding author

Abstract

An interferon-inducible gene, 2'-5'-oligoadenylate synthetase-1 (OAS1), plays an essential role in uterine receptivity and conceptus development by controlling cell growth and differentiation in addition to its anti-viral activities. However, the specific part of OAS1 is not yet documented in the goat. Therefore, in the present study, the coding sequence (CDS) of the OAS1 gene was amplified, sequenced and characterized through various Bioinformatics tools. Its temporal expression profile was also examined in the endometrium of caprine (cp) for the first time. A fragment of the cpOAS1 gene, 890 bp in length, was amplified from complementary DNA (cDNA). Nucleotide and deduced amino acid sequences revealed 99.6 to 80.4 % and 99.3 to 72.3 % identities with that of ruminants and non-ruminants, respectively. A constructed phylogenetic tree revealed that sheep and goats belong to the same clade but differ from large ruminants. Besides the Physico-chemical characteristics, its localization, various posttranslational modifications, immunogenic sites, possible domains, various motifs, and interactions with other probable proteins were predicted. In addition to the secondary structure, the three-dimensional structure was predicted using homology modelling servers and a refined model, generated by the Swiss model was the best one as based on stereochemistry validated with different programs. Further, relative expression of cpOAS1 mRNA and protein was determined by quantitative real-time PCR (qPCR) and western blot, respectively, in the endometrium of pregnant and cyclic does. Caprine OAS1 protein (42/46kDa) was detected in the endometrium of pregnant and cyclic does. Both cpOAS1 mRNA and protein were expressed maximally ($P<0.05$) in the endometrium during pregnancy as compared to cyclic does. It is concluded that the cpOAS1 sequence is conserved and integrative Bioinformatics analysis provides a sound foundation for further structural and functional characterization of cpOAS1 protein in the establishment of pregnancy in goats.

KEY WORDS Goat, Endometrium, OAS1, Embryo survival

1 INTRODUCTION

Orientation and connection of trophectoderm of the migrated blastocyst to the luminal epithelial surface of the uterus is the critical period to harmonize the implantation cascade[1]. In this period, embryo mortality is most prevalent in all domestic ruminants[2,3] and may be due to deficiencies attributed to immune functions, uterine functions, inappropriate conceptus development, and implantation[4,5]. Mononuclear cells of trophoectoderm of a preimplant embryo produces and release interferon tau (IFNT) between 11 to 24 day of pregnancy in ruminants[5,6]. This IFNT binds to the Type-1 IFN receptor (IFNR) located on luminal epithelial cells of endometrium[7] and exerts its anti-luteolytic activity by different mechanisms[8]. Interferon tau induces and up-regulates the expression of several genes in the endometrium during pregnancy including 2'-5'-oligoadenylate synthetase-1 (OAS1)[9,10,11].

The mammalian 2'-5' oligoadenylate synthetases (2'-5'OASs) are enzymes that play a crucial role in mediating resistance to virus infection, control of cell growth, differentiation, and apoptosis[12,13,14]. It binds to double-stranded RNA and catalyzes the polymerization of ATP into 2'-5'-linked oligoadenylates which activate a constitutively expressed latent endonuclease, RNase L, to block viral replication and initiate apoptosis in some cell types. The mammalian OAS genes have undergone multiple gene duplication events resulting in three size classes of enzymes: small (40/46-kDa isoforms), intermediate (69/71-kDa isoforms), and large (100-kDa)[15,16,17,18,19]. The biological significance of these multiple OAS forms is unknown, but each has distinct subcellular locations and functional differences in activation requirements and catalytic parameters[17,20,21,22]. This protein is associated with different subcellular fractions such as mitochondrial, nuclear, and rough/smooth microsomal fractions.

OAS1 is the novel and most abundant gene expressed in cyclic and increased the level during early pregnancy in the endometrium of bovine and ovine, and is regulated by *IFNT* and progesterone[9,11,23]. Its level increases in the endometrium during early pregnancy and plays an important role in antiviral responses, control of cellular growth and differentiation for successful implantation, and pregnancy establishment in bovine and ovine[9,10,11]. In addition, intrauterine administration of IFNT along with progesterone stimulates OAS expression in the cyclic endometrium of the animals and/or in-vitro culture endometrial cells[10,11]. Even though the OAS1 is involved in uterine receptivity, implantation, and survivability of the embryo, it has not yet been studied in goats (*Capra hircus)* except one predicted sequence is available in NCBI (GenBank Acc. No. XM_005691488).

Goat (*Capra hircus*) being a multi-functional animal and commonly known as the poor man's cow, acts as a source of crop insurance and supplementary income along with nutritional security for lower, poor and marginal farmers in South Asian countries, especially in India[24]. The goat sector contributes 8.4 % to India's livestock gross domestic product (GDP) through meat, milk, skin and manure[25]. Considering the important role of OAS1 in uterine receptivity and embryonic survival, in addition to its antiviral function, the present work was undertaken to amplify, sequence, characterize, analyze the integrative bioinformatics and elucidate expression patterns in goat endometrium.

2 MATERIALS AND METHODS

2.1 Experimental design and collection of samples

All procedures and samples used in the present study were approved by the Institutional Animal Ethics Committee (IAEC; proposal no. AGB/PG-1/14-15). For molecular characterization and expression profile of the cpOAS1 gene, freshly slaughtered uteri were collected from the local slaughterhouse, Bhilai, Chhattisgarh immediately after exsanguination. Collected uteri were divided into two groups i.e. pregnant (n=12) and non-pregnant (n=6). Pregnant uteri were further classified into two subgroups, early pregnant (n=6, 16 to 24 d) and late pregnant (n=6, 25 to 40 d). Based on crown-rump length measurement, the number of days of pregnancy was determined[26]. These samples were processed as per the method described earlier[27].

2.2 RNA isolation, cDNA synthesis, amplification, sequencing and characterization of cpOAS1 gene

For amplification and mRNA expression of the cpOAS1 gene, total RNA isolation and cDNA synthesis were carried out. Total RNA was isolated from 50 mg of collected endometrial tissue using Tri reagent (Sigma, USA) as per the manufacturer's instructions. The quality and integrity of RNA were checked by agarose gel electrophoresis and the quantity of total RNA was measured by a Qubit 3 Fluorometer (Invitrogen, USA). Further, cDNA was synthesized using total RNA (2μg) by the Revert Aid first-strand cDNA reverse transcription system (Fermentas, USA). After the termination of cDNA, each cDNA preparation was diluted four times with nuclease-free water and stored at -20°C till further use.

A pair of degenerate primers was designed based on a predicted sequence (accession number XM_005691488) and used for amplification of the cpOAS1 gene (Table 1). PCR amplification was carried out in a total volume of 25 μl of reaction mixture containing 20 pM of each primer and 5μl diluted cDNA by using a 2x master mixture (Sigma, USA) in a thermal cycler (Bio-Rad, USA). The PCR protocol included an initial denaturation at 94°C for 4 min followed by 34 cycles of denaturation (94°C for 30 s), annealing (56°C for 30 s) and extension (72°C for 1 min) followed by one cycle of final extension (72°C for 10 min). The PCR product was resolved by agarose gel (0.7%) electrophoresis and visualized by SYBR safe gel staining (Invitrogen, USA) under the Gel-Doc system (Molecular image XR^{+}, Bio-Rad, USA). The amplified product was purified by using the HiPurA^{TM}PCR product purification kit (Himedia Laboratories, India) as per the manufacturer's instructions. Purified PCR product was sent for forward and reverse sequencing using an ABI PRISM automatic sequencer under standard cycle conditions of Sanger's dideoxy chain termination method. These sequences were subjected to BLAST analysis (www.ncbi.nlm.nih.gov/BLAST). The nucleotide and the deduced amino acid sequences were aligned with others sequences of various species. Pairwise identity and phylogenetic evolutionary analysis were conducted using the DNA Star tool.

2.3 Integrative bioinformatics analysis of cpOAS1 protein

2.3.1 Sequence retrieval and Physico-chemical parameters of cpOAS1

The submitted and published cpOAS1 (Acc No MN564841) template from the present study was used for bioinformatics analysis. This template was blasted against the PDB database using Blast P in NCBI Blast, using default parameters. Monomer porcine (PDB ID: 4rwp) template was selected based on maximum identity among the amino acids, e-value, query coverage and other properties. This template was used for predicting the 3-D structure of the cpOAS1 protein. ProtParam tool of ExPASy, SIB Bioinformatics resource portal (http://web.expasy.org/protparam/), was used to compute the basic Physico-chemical properties of cpOAS1 like molecular weight, theoretical isoelectric point (pI), the total number of positive (Asp + Glu) and negative residues(Arg + Lys), formula, number of atoms, extinction coefficient (EC)[28], estimated half-life[29], instability index (II)[30], aliphatic index (AI;)[31] and grand average hydropathy (GRAVY)[32]. The Kyte-Doolittle scale was used for detecting hydrophobic regions in the cpOAS1 proteins. Regions with positive and negative values are depicted as hydrophobic and hydrophilic, respectively. Under this scale, the window size was kept at 9, the relative weight for window edges was 100 % and the linear weighted variation model was selected. Hydrophobicity was computed by the ProtScale.

2.3.2 Subcellular localization, structure, function and various properties of cpOAS1 protein

Subcellular localization was predicted by PSORT II (https://psort.hgc.jp/form2.html). Subcellular localization of cpOAS1 protein was also confirmed by using deep learning (Neural networks algorithm) by the DeepLoc-1.0 server (https://services.healthtech.dtu.dk/service.php?DeepLoc-1.0). Signal peptide was evaluated using SignalP 5.0[33](https://services.healthtech.dtu.dk/service.php?SignalP-5.0) and further confirmed by Signal-3L 3.0 (http://www.csbio.sjtu.edu.cn/bioinf/Signal-3L/). The transmembrane helices were analyzed by the TMHMM server v. 2.0[34](https://services.healthtech.dtu.dk/service.php?TMHMM-2.0). The secondary structural feature of cpOAS1 protein was computed by the SOPMA (Self Optimized Prediction Method with Alignment)[35]software by keeping window width 17 and threshold 8 (https://npsa-prabi.ibcp.fr/cgibin/npsa_automat.pl?page=/NPSA/npsa_sopma.html). The accessible

surface area (ASA), structure, disorder, and phi/psi dihedral angles of amino acids were predicted by the NetSurfP2.0 server[36](https://services.healthtech.dtu.dk/service.php?NetSurfP-2.0). Rossmann fold sequence domains and their specificity for the cofactors FAD, NAD or NADP were predicted by Cofactory - 1.0[37](https://services.healthtech.dtu.dk/service.php?Cofactory-1.0). Anti-oxidative properties of cpOAS1 were predicted by AnOxPePred - 1.0 tool using convolutional neural network[38](https://services.healthtech.dtu.dk/service.php?AnOxPePred-1.0).

2.3.3 Immunological features of cpOAS1

cpOAS1 B cell epitopes (BepiPred Linear Epitope Prediction 2.0) and T cell epitopes (immunogenicity prediction) with a 50% threshold were predicted using IEDB analysis. Under the BepiPred-2.0 server, a random forest algorithm trained on epitopes and non-epitope amino acids determined from crystal structures was used.

2.3.4 Prediction of post-translational modifications (PTMs) in cpOAS1

Online prediction servers available at the center for biological sequence analysis (CBS), Technical University of Denmark (http://www.cbs.dtu.dk/) were used to predict C-mannosylation sites (NetCGlyc 1.0 server)[39], N-terminal acetylationsites[40] (NetAcet 1.0 server), glycosylphosphatidylinositol anchoring[41](GPI-anchoring or glypiation; NetGPI-1.1 server), N-linked glycosylation sites (NetNGlyc1.0 server; http://www.cbs.dtu.dk/services/NetNGlyc/), mucin-type GalNAc O-glycosylation sites[42] (NetOGlyc - 4.0), Glycation of amino groups of lysines[43] (NetGlycate 1.0 server), phosphorylation sites[44] (both generic and kinase-specific predictions; NetPhos-3.1 server) and arginine and lysine propeptide cleavage sites[45] (ProP 1.0 server). Prediction of acetylation on internal lysines (PAIL) of cpOAS1 protein was done using PAIL software[46]. The fourth-generation GPS algorithm integrated with the particle swarm optimization (PSO)[47] method was employed for the prediction of sumoylation sites in the cpOAS1 protein. Disulfide bridges were predicted in the cpOAS1 protein sequence using CYS_REC (http://www.softberry.com/cgi-bin/programs/propt/cys_rec) tool.

2.3.5 Computational modeling of three-dimensional (3-D) structure of cpOAS1 protein

The three-dimensional model was generated using MODELLER 10.1 (https://salilab.org/modeller/), SWISS-MODEL (https://swissmodel.expasy.org/), PHYRE2 (http://www.sbg.bio.ic.ac.uk/phyre2/html/page.cgi?id=index) and GENO3D (https://geno3d-prabi.ibcp.fr/cgi-bin/geno3d_automat.pl?page=/GENO3D/geno3d_home.html) software. In MODELLER 10.1, the 3-D structure was predicted as per the described procedure[48]. During this procedure, five three-dimensional structures were generated using 4 rwp as the template. The best possible structure was selected considering the DOPE (Discrete Optimized Protein Energy) score. SWISS-MODEL software was used to generate a refined 3-D model of the cpOAS1 protein. Generated cpOAS1 model was predicted sequentially with the global model quality estimate (GMQE) and the QMEAN score[49]. Intensive modeling mode was used to predict the 3-D structure using protein homology/analogY recognition engine V 2.0 (PHYRE2)[50]. In this model, the template was selected based on heuristics to maximize confidence, percentage identity and alignment coverage. In GENO3D, out of five models, the low energy model was selected for evaluation and further validation[51]. All 3-D structures of the cpOAS1 protein generated by all the four types of software/server were then evaluated to test the structural integrity through various online model evaluation servers included Errat[52], PROCHECK[53] and VERIFY3D[54]. Ramachandran plot as evaluated by PROCHECK was generated to check the stereochemical properties of cpOAS1 protein structure which has been modeled[55]. In this plot, structural validation was done by evaluating the number of amino acid residues in favoured regions, allowed regions and disallowed regions. Graphical inspections and similarity of the generated P2 model with the template model (4rwp) were done using UCSF Chimera[56](http://www.cgl.ucsf.edu/chimera/). Different protein models were viewed in the RasMol.

2.3.6 Domains architectures, linear motifs, protein interactions and biding sites

Domains compositions of cpOAS1 were predicted in Pfam (version 34.0), InterPro (version 85.0) and SMART

(Simple Modular Architecture Research Tool)[57] database. Linear motif and functional characterization were done using the eukaryotic linear motif (ELM) prediction tools. Proteins that interact with caprine OAS1 were predicted by the String (Version 11.0) program (http://string-db.org) and the cpOAS1 sequence was used to search against the *Ovis aries* organism and the confidence score was set to high (0.700). Different metal biding, active and NTP binding sites were predicted by the InterPro database.

2.4 Expression of cpOAS1 mRNA using quantitative real-time PCR (qPCR)

For qPCR of cpOAS1, primers pairs of OAS1 and Beta-actin (ACTB) genes were used as described in Table 1. ACTB gene was used as an endogenous control. Quantitative real-time PCR was carried out in CFX-96 Real-Time PCR System (BioRad, USA). Primer concentration was optimized using the primer matrix experiments for valid transcript quantification[58]. All qPCR reactions were performed in duplicates in a volume of 20 µl. The reaction mixture contained 10 pM of each gene-specific primer, 2 µl of cDNA template, 1×SYBRGreen PCR master mix (Sigma, USA) and nuclease-free water to make the total reaction volume of 20 µl. Cycling conditions of PCR were initial denaturation for 10 min at 95°C, followed by 40 cycles of denaturation for 30 s at 95°C; annealing and extension for 60 s at 60°C. The specificity of the amplified product was checked by running a dissociation curve. Mean threshold cycle values (C_T) for genes under study were calculated for duplicate samples and relative transcript abundance for target gene expression was calculated using the formula $2^{-(\Delta\Delta^{\hat{}}_T)}$[59].

2.5 Expression of cpOAS1 protein using western blotting

Caprine OAS1 proteins expressed in goat endometrial cells were separated on a 12% SDS-PAGE gel and transferred electrophoretically to a PVDF membrane (Biotrace^{TM} PVDF, PALL Corporation, India) at 100 V for 2 h uteri as described earlier[58]. After transfer, the membrane was incubated in blocking buffer [5% (w/v) skim milk powder in PBS, pH 7.4] at room temperature for 1h with gentle agitation. To detect the cpOAS1 isoform proteins expressed in the goat endometrium, the membranes were incubated with rabbit OAS1 polyclonal antibody (Invitrogen, Catalog # PA5-41755) in 1:800 dilutions in blocking buffer at 4@C overnight. To detect overexpressed cpOAS1 isoforms, the membranes were incubated at room temperature for 1.5 h with HRP conjugated mouse anti-rabbit secondary antibodies (Santa Cruz, CA, USA) to a 1:2000 dilution of in PBS. DAB substrate buffer system (GeNei, India) was used to detect the presence of secondary antibody. The densitometric analysis of protein was performed by NIH ImageJ 1.44p software (National Institutes of Health, Bethesda, Maryland, USA). The relative intensity of the bands was quantified and normalized with β-actin (Santa Cruz, CA, USA).

2.6 Statistical analysis

Relative abundance values for cpOAS1 mRNA and protein expression were analyzed using SPSS software (version 2015). Differences of means across stages were analyzed using a one-way analysis of variance followed by the Duncan's Multiple Range Test (DMRT). Results were expressed as mean± standard error of the mean and the significance of differences between means was determined at a 5% level of significance ($P< 0.05$).

3 RESULTS

3.1 Amplification, sequencing and characterization of cpOAS1 gene

A fragment of a single specific and expected 890 bp in length was amplified and sequenced (FIGURE 1S). Accordingly, the nucleotide sequence of the cpOAS1 gene was submitted to GenBank for non-descript Anjori goat with accession number (MN564841). The comparison of nucleotide and amino acid sequences of cpOAS1 with available OAS1 sequences of *Capra hircus* (predicted), *Ovis aries*(predicted), *Bos taurus* (predicted), *Bubalus bubalis* ,*Bison bison* (predicted), *Bos mutus* and *Sus scrofa*confirmed the cpOAS1 gene (FIGURE 2S and 1). Complementary DNA (cDNA) sequence of cpOAS1 shared 99.6, 96.1, 94.4, 94.3, 95.2, 94.6, 94.4, 80.6 and 80.4 % with *Capra hircus* (predicted), *Ovis aries*(predicted), *Bos indicus* (predicted), *Bos taurus* ,*Bubalus bubalis* , *Bison bison* (predicted), *Bos mutus* , *Sus scrofa* and *Equuscabalus* , respectively (FIGURE 3S). Deduced amino acid sequence of cpOAS1 shared 99.3, 92.6, 89.9, 89.9, 91.2, 90.2, 88.9, 72.3 and 75.0%

identity with *Capra hircus* (predicted), *Ovis aries* (predicted), *Bos indicus*(predicted), *Bos taurus* , *Bubalus bubalis* , *Bison bison* (predicted), *Bos mutus* , *Sus scrofa* and *Equus cabalus* , respectively (FIGURE 4S).

3.2 Phylogenetic evolution

Phylogram revealed the dissemblance of *Sus scrofa* and *Equus cabalus* OAS1 from that of ruminants during evolution. Subsequently, ruminant homologues are divided into two subclades of small (*Ovis aries* and *Capra hircus*) and large (*Bos indicus* and*taurus* , *Bubalus bubalis Bos bison* , *Bos mutus*) ruminants. In small ruminants, *Ovis aries* and *Capra hircus* belong to different clusters (FIGURE 2).

3.3 Integrative bioinformatics analysis of cpOAS1 protein

3.3.1 Sequence retrieval and Physico-chemical parameters

Various physical and chemical parameters were computed by ProtParam, which are shown in Table 2. Results of ProtScale showed that many hydrophilic amino acids are present in the cpOAS1 protein, which form hydrophilic regions and the proteins. Maximum and minimum scores were 1.656 (position number 25) and -2.678 (position number 37), respectively (FIGURE 3).

3.3.2 Subcellular localization, structure, function and various properties of cpOAS1 protein

cpOAS1 protein is possibly multi-located but dominates in the cytoplasm and is a soluble protein (FIGURE 4 and Table 3) based on the result of PSORT II and DeepLoc-1.0 servers. Based on the signal peptide prediction using SignalP 5.0 server and Signal-3L 3.0 engine, there were no signal peptide and cleavage sites in the cpOAS1 protein (FIGURE 5SA). Transmembrane of TMHMM results showed that there is no predicted transmembrane helix in the sequence of cpOAS1 (FIGURE 5SB). Prediction of the secondary structure of cpOAS1 protein by the SOPMA revealed that the alpha helix (43.92%) is dominated followed by the random coil (39.86%), extended strand (13.85%) and beta-turn (2.36%) and percentage of other structures like Pi helix, Beta Bridge, Beta region, ambiguous states, etc. were zero (FIGURE 6S). Based on NetSurfP, it was found that the cpOAS1 protein has a combination of buried and exposed amino acid residues (FIGURE 5). The relative surface accessibility (RSA) value was ranged from 0.004 to 0.840 and absolute surface accessibility (ASA) was 0.672 to 151.586. Maximum disorders residues were present at the C-terminal end (FIGURE 5). Rossmann fold sequence domains and their specificity for the cofactors FAD, NAD or NADP were not found in the cpOAS1 protein (FIGURE7S). Various sequences, which show anti-oxidative properties, were found in the cpOAS1 (Table 4).

3.3.3 Immunological features of cpOAS1

B cell epitope prediction (Bepipred Linear Epitope Prediction 2.0) using IEDB analysis indicated that there are 14 potential immunogenic sites in the cpOAS1 which can act as antigen while, with a 50% threshold, seven sites act for T cell epitope (immunogenicity prediction) given in Table 5 and Figure 8S. The residues with scores above the threshold (0.5) are predicted to be part of an epitope and colored in yellow on the graph (where Y-axes depict residue scores and X-axes residue positions in the sequence).

3.3.4 Post-translational modifications (PTMs)

C-mannosylation sites and N-terminal acetylation sites were not found in the cpOAS1 protein (FIGURE 9S). cpOAS1 is a non-GPI-anchor protein (FIGURE 9S). Based on the analysis of the NetNglyc server, a potential N-linked glycosylation site was not found in the cpOAS1 protein (FIGURE 9S). Potentially two predicted mucin type GalNAc O-glycosylation sites were found in the cpOAS1 (FIGURE 6A). Nine glycation sites at amino groups of lysine residue were present in the cpOAS1 protein and these sites are shown in Figure 6B. Various predicted phosphorylation sites in the cpOAS1 protein sequence are shown in Table 6 and Figure 9S. In the cpOAS1,14-serine, 8- threonine and 1-tyrosine residues were found. One potential arginine and lysine propeptide cleavage site was predicted in the cpOAS1 (Data not shown). Different 10 internal acetylation sites by PAIL software were predicted in the cpOAS1 (Table 7). Sumoylation sites in the cpOAS1 protein under the medium threshold were presented in Table 8. In the cpOAS1, two sumoylation sites at 62 and 280

positions were found. and eight cysteines are found at positions: 53, 122, 134, 164, 190, 215, 240 and 277. The two most probable pattern of pairs 134-277, 164-190, were found using the CYS_REC tool.

3.3.5 Computational modeling of three-dimensional (3-D) structure of cpOAS1 protein

The best possible 3-D structure of cpOAS1 obtained from MODELLER 9.18, SWISS-MODEL, PHYRE 2 and GENO3D were designated as P1, P2, P3, P4, respectively (FIGURE7). These models were evaluated and their results are shown in Table 9. Based on Errat, PROCHECK and VERIFY3D validations, the model generated by SWISS-MODEL was found to be the best model for the prediction of cpOAS1 protein structure. The overall quality of model P2 determined by ERRAT value (96.35%) and VERIFY3D score (92.81%) was the highest and the stereo-chemical properties checked by PROCHECK were found to be the best among all the four models (Table 9). Model P2 along with its Ramachandran Plot (FIGURE 8) showed that there were 94.6 % residues in the most favoured region and 5.4 % additional allowed regions (%) and none in the disallowed region. Further, in the P2 model, global model quality estimation (GMQE) and qualitative model energy analysis (QMEAN) values were 0.86 and 0.26, respectively, which are in the acceptable range. In the P2 model, the GMQE score reflects the expected accuracy of that alignment and is expressed as a number between 0 and 1 where higher numbers indicate higher reliability. The QMEAN is a composite scoring function describing the major geometrical aspects of protein structures. Result of the superimposition of the P2 model and porcine (4rwp) generated in UCSF Chimera and the ProSA-web web server indicated that the P2 model was almost similar in structure (FIGURE 8B). The Z-score of the P2 model was found to be -8.32 which was within the range of porcine OAS protein (-10.09), the best template (4rwp; FIGURE 10S).

3.3.6 Domains architectures, linear motifs, protein interactions and biding sites

Various domains with their locations were searched in Pfam (version 34.0), InterPro (version 85.0) and SMART (Simple Modular Architecture Research Tool) database and are presented in Table 10. Eukaryotic linear motifs found that there are 51 different types of motifs and 120 instances recognized by the different amino acid sequences in the protein (FIGURE 9). These motifs functionally characterize the major portion of cpOAS1 protein which is involved in the cell signaling processes and have various kinase and phosphorylation sites. The probable protein-protein interactions in which cpOAS1 protein might participate were analyzed using the STRING 11.0 tool. The top 10 proteins that interacted with OAS1 were Myxovirus Resistance 1 (MX1), Ubiquitin Specific Peptidase 18 (USP18), DExD/H-Box Helicase 58 (DDX58), RAB Guanine Nucleotide Exchange Factor 1 (RABGEF), Radical S-Adenosyl Methionine Domain Containing 2 (RSAD2), Interferon stimulated gene 17 (ISG17), Interferon regulatory factor 7 (IRF7), 2'-5'-oligoadenylate synthetase 2 (OAS2), Interferon Induced Protein with Tetratricopeptide Repeats 1 (IFIT1) and interferon-induced with helicase C domain 1 (IFIH1; FIGURE10). All the 10 predicted interactions had good scores ranging from 0.880 to 0.789 (Table 11). In the cpOAS1, three metal-binding triads, 16 active sites and eight NTP binding sites were predicted (Table 12.).

3.4 Expression of cpOAS1mRNA

Constitutive expression of cpOAS1 mRNA was detected in pregnant and non-pregnant endometrium of does. Relative mRNA transcript abundance of cpOAS1 gene was significantly ($P<0.05$) higher during pregnancy (days 16 to 40 as compared to cyclic does (FIGURE 11). The mean fold change in cpOAS1 mRNA was 10.34 and 3.96 fold greater ($P<0.05$) during early and later stages of pregnancy, respectively, as compared to cyclic does (FIGURE 11.). cpOAS1 gene showed a single peak in the dissociation curve indicating specificity of qPCR reaction and it also signified that primer was highly specific to the target and had no primer dimer formation (FIGURE 11S).

3.5 Expression of cpOAS1 protein

The informative mRNA level of the cpOAS1 gene was further validated and quantified at the protein level in the endometrium of does by the western blot technique. Caprine OAS1 protein (˜46 kDa, 69/71 kDa) was detected in pregnant and non-pregnant endometrium of does (FIGURE 12) but approximate, ˜42 kDa

in size was detected only in early pregnancy of does. The cpOAS1 protein level (69 kDa) was significantly high ($P<0.05$) during early pregnancy (16 to 24 d) and later stage of pregnancy (25 to 40 d) as compared to the non-pregnancy stage. Relative expression of cpOAS1 protein was 6.73 and 2.98 fold higher during early and later stages of pregnancy, respectively, as compared with non-pregnant does (FIGURE 12). Beta-actin was used as endogenous control and it showed an equal intensity of 43 kDa protein in all three groups (figure not shown).

4 DISCUSSION

To the best knowledge, the present study is the first instance in which OAS1 was amplified, sequenced, characterized, analyzed by integrated Bioinformatics, and expression pattern was also studied in the endometrium of local goats (Anjori goats).

Caprine OAS1 displayed the highest sequence homology with the predicted *Capra hircus* and *Ovis aries* sequences followed by other species. This analysis indicated that the cpOAS1 sequence is conserved in mammals. But some nucleotide differences lead to changes in amino acid composition which can lead to different properties with other species. OAS1 protein has been characterized as an innate immunity gene in different species[60,61,62] but no report has been there on its structural and functional prediction in goats.

In the present study, the instability index of cpOAS1 is predicted to a very unstable as the value is greater than 40, which indicates that it is not suitable for *in vitro* heterologous expression system[30]. The calculated AI of the cpOAS1 protein is 81.96 which indicates its stability at higher temperature[31]. The negative GRAVY value of cpOAS1 protein indicates that it is a protein consisting of more hydrophilic residues which may be a clue towards its secretory nature. The theoretical pI value of cpOAS1 indicates that it is basic and useful for wet lab extraction (through chromatographic methods). The half-life of cpOAS1 is 1.3 hours which will be helpful in the estimation of the residual time of this protein after its expression in any system. These structural and physicochemical properties of the cpOAS1 may be used for predicting protein structural and functional classes[63,64], protein-protein interactions[65], subcellular locations[66], peptides of specific properties[67], microarray data[68] and protein secondary structure[69].

Membrane proteins usually have one or more transmembrane segments, which are very hydrophobic making the chances for crystallization of membrane proteins small[70,71]. The absence of transmembrane helix and signal peptides in the cpOAS1 protein sequence suggests that the cpOAS1 gene encodes a hydrophilic, secretory protein. This also suggests that the protein is not destined to be transported across the membrane and hence localized in the cytoplasm. Results of ProtScale also additionally showed that many hydrophilic amino acids are present in the cpOAS1 protein.

cpOAS1 protein was predicted as multi-located but dominantly in the cytoplasm. Moreover, its subcellular localization was additionally confirmed to be the cytoplasmic protein. Furthermore, the different variants of OAS protein were also found in the cytoplasm and mitochondria[72,73] which also supports the current *in silico* analysis of this protein to its subcellular localization. The secondary structure of cpOAS1 revealed the domination of alpha-helix in cpOAS1 which indicates folding energy for right-handed is more favorable. Therefore, primary and secondary structure prediction was very useful in predicting the interaction of OAS1 with other molecules like RNAase L (innate immunity role) and IFNT which leads to its release during viral infection as well as conceptus implantation[74]. Solvent exposed vs. non-exposed amino acid residues have an important role in determining the protein structure[75]. The presence of buried and exposed amino acid residues in the cpOAS1 signifies the presence of transmembrane segments in this protein. Surface accessibility (SA) or solvent accessible surface area (SASA) of proteins has always been considered the main feature for determining protein folding, packaging and stability[76]. The current study revealed the different immunogenic B cell epitopes and conformational epitopes in the cpOAS1. These regions represent a strong indicator of the antigenic nature of these proteins which can be used for vaccine/antibody and immunotherapy development[77,78,79].

Many eukaryotic proteins require multiple protein translational modifications (PTMs) to reach a native, biologically active conformation and should be considered as the major determinants for successful protein

synthesis in addition to the physio-chemical and structural features of amino acid sequences[80]. In the present study, different PTMs were predicted. The presence of two mucin type GalNAc O-glycosylation sites in the cpOAS1 indicates its role in protein sorting, immune recognition, receptor binding, folding, stability as well as serving regulatory functions[81,82]. The identification of nine glycation sites in the cpOAS1 protein may be helpful to understand the biological function of protein glycation and identification of the associated disease treatment[43,83]. The presence of 21 phosphorylated sites in the cpOAS1 indicates its roles in the regulation of many cellular processes, including cell cycle, growth, apoptosis and signal transduction pathways[84]. The presence of one arginine and lysine propeptide cleavage site in the cpOAS1 indicates that this protein undergoes for post-translational processing to become biologically active polypeptides[45]. The presence of internal acetylation sites in the cpOAS1 protein orchestrates a variety of cellular processes, including transcription regulation[85,86], DNA repair[87], apoptosis[88,89], cytokine signaling[90], and nuclear import[91], etc. The presence of two SUMOylation sites in the cpOAS1 indicates that it is involved in the regulation of gene expression, cellular signaling, immune responses and the maintenance of genomic integrity[92]. The presence of cysteine disulfide bridges in the cpOAS1 provides proper folding, stability and more suitability for eukaryotic expression system than prokaryotic system[93].

The tertiary structure of proteins refers to the overall three-dimensional shape and this included polar, nonpolar, acidic, and basic R groups that exist on the protein. In the present study, the Ramachandran plot shows that residues fell in the most favored, allowed and disallowed regions in the model (P2) generated by SWISS-MODEL were the most favored cpOAS1 3-D structure. It indicated that the refined model may be a true reflection of an experimentally-obtained OAS1 protein structure of goat. This computationally predicting 3D structure of cpOAS1 protein may be helpful for drug screening and drug design, designing mutagenesis experiments, detecting active sites, solving the phase problem by molecular replacement, and understanding the effect of disease-associated mutations[74,94]. This 3-D structure is also useful to evaluate the conformational differences with other species, its cross-reactivity and deciphering the activity of protein during different interactions with molecules[95].

Protein domains are the fundamental units of protein structure, folding, function, evolution and design[96],[97]. Out of various domains in cpOAS1, the OAS1_C domain is one of the important domain and is the largely alpha-helical, C-terminal half of 2'-5'-oligoadenylate synthetase 1, being described as domain 2 of the enzyme and homologous to a tandem ubiquitin repeat. It carries the region of enzymic activity between 320 and 344 at the extreme C-terminal end[98]. Oligoadenylate synthetases are antiviral enzymes that counteract viral attacks by degrading viral RNA. The enzyme uses ATP in 2'-specific nucleotidyl transfer reactions to synthesize 2'-5'-oligoadenylates, which activate latent ribonuclease, resulting in degradation of viral RNA and inhibition of virus replication. The 2'-5' OASs are also implicated in cell growth control, differentiation, and apoptosis[99],[100]. This domain is often associated with the NTP_transf_2 domain. In vertebrates, 2'-5' OASs (2'-5'-oligoadenylate synthetases) are induced by interferon during the innate immune response to protect against RNA virus infections. Nuclear factors NF90 and NF45 dimerize through their common DZF domain and form a protein complex that is involved in a variety of cellular processes and affects the replication of several viruses through direct interactions with viral RNA. Eukaryotic linear motifs (ELMs) are compact protein interaction sites and these provide a wide range of functionality to proteins[101,102]. The presence and characterization of ELM in cpOAS1 may be useful to our understanding of both the physiological and disease states of the cell. Recognition of 51 different types of motifs and 120 instances in the cpOAS1 may be helpful in the identification of different parts of cpOAS1 protein which is involved in cell signaling processing and its interaction with other molecules.

In the present study, cpOAS1 interacted with different molecules. All the 10 predicted interactions indicate a reliable interaction among them (Table 11). The proteins DDX58, RSAD2, ISG17, IRF7, IFITI and IFIH were known to have directly or indirectly in antiviral activity and immunity development like OAS1, and the rest were either uncharacterized or had different functions (Table 11). Such networks may be useful for filtering and assessing functional genomics data and for providing an intuitive platform for annotating structural, functional and evolutionary properties of cpOAS1 proteins. These predicted interaction networks can also suggest new directions for future experimental research and provide cross-species predictions for

efficient interaction mapping[103].

In the present study, the presence of basal cpOAS1 transcript and protein in cyclic endometrium of does is harmonious with the expression of OAS gene in the endometrium of bovine[9,11] and ovine[11,23]. The presence of the OAS1 in non-pregnant endometrium indicates that it may be involved in normal uterine development by creating an anti-viral environment during the estrous cycle. It has been found that during the estrous cycle, the endometrial cellular content of 2-5(A) synthetase may have a role in regulating luteolysis[10] and also have an inverse relationship with PGF2 secretion in IFNT-treated bovine uterine explants[104].

In agreement with our study, a higher level of cpOAS mRNA and protein was also observed in the endometrium during the early stage of pregnancy (13 to 25 days) in bovine[9,10] and ovine[11,23]. The expression of OAS1 mRNA is parallel with conceptus elongation and IFNT secretion during early pregnancy between 16 to 21 days in does[105,106], and 11 to 21 d in ewes and cows[107]. Some studies have also found that intrauterine infusion of IFNT in cyclic ewes and cows, and*in-vitro* culture of different types of endometrial cells supplementation with IFNT increases the OAS expression or its activity[10,11]. Moreover, different ovine endometrial cell lines expressed the different isoforms of OAS (40/46, 69/71 and 100-kDa). Three distinct classes of 2-5A synthetases have been described that correspond to proteins of 40-46 kDa, 69-71 kDa, and 100 kDa. The 40 and 46 kDa forms are produced by alternative splicing of the same gene. The 69 and 71 kDa forms are also produced by alternative splicing of a gene and consist of two adjacent homologous domains whose sequences are highly similar to that of the 40/46 kDa forms[19,99]. Because the three major OAS forms are generated from independent genes, each OAS gene likely has different response elements in its promoter, which may account for the differential effects of types I and II IFNs on the OAS gene transcription[15,16,17,108]. Various forms especially the 40/ 46- and 69/71-kDa isoforms of OAS induced by IFNT are likely to have a physiological role in the endometrium during early pregnancy in sheep and cows[10,11]. The exact mechanism of endometrial OAS in the establishment of pregnancy in ruminants is still clearly unknown. But it is believed that the OAS system is implicated in the antiviral response and regulation of ISG expression in response to IFNs or viral infection as well as cell growth, differentiation, and apoptosis[12,14,23,108]. Present findings and other studies advocate that various OAS-mediated cellular events could contribute to endometrial function during the establishment of pregnancy in ruminants[109, 110].

5 — CONCLUSION

In conclusion, this study reports the molecular characterization Bioinformatics analysis and expression profile of the cpOAS1gene. Molecular description of the coding region of cpOAS1 would provide an opportunity to explore SNP markers and their association with goat reproduction potential. The prediction of structural, physicochemical, functional and immunological properties is a good indicator of expression in an heterologous system. Detection of the increased level of cpOAS1 mRNA and protein in the endometrium during pregnancy suggests its probable function in the antiviral response as well as cell proliferation, growth and differentiation during pregnancy. Nevertheless, these studies warrant further investigation to locate the OAS1 in uterine endometrium and to know the exact role of OAS1 together with other isoforms of the OAS gene in the conceptus implantation and placentation in does.

ACKNOWLEDGMENTS

The work was supported under the Science and Engineering Research Board (SERB), Department of Science and Technology (DST) funded project (SB/YS/LS-27/2014), Government of India, New Delhi, India to Dr. Asit Jain.

DECLARATION OF INTEREST

The authors declare no conflict of interests and have no financial or personal relationship(s) with other people or organizations which could inappropriately influence the write-up of this paper

AUTHORSHIP

Asit Jain and Tripti Jain conceptualized, designed and drafted the manuscript. Asit Jain, Tripti Jain and Khushboo Chandrakar conducted the experiments. Kishore Mukherjee and Sita Prasad Tiwari contributed in analyzing the data, editing the MS and providing facilities. All authors approved the final draft of the manuscript.

DATA AVAILABILITY STATEMENT

The data that support the findings of this study are available from the corresponding author upon reasonable request

REFERENCES

1. Burghardt RC, Bowen JA, Newton GR, Bazer FW. Extracellular matrix and the implantation cascade in pigs. *J Reprod Fertil.*1997;52:151-164.
2. Spencer TE, Bazer FW. Conceptus signals for establishment and maintenance of pregnancy. *Reprod Biol Endocrinol.* 2004:2:1-15.
3. Diskin MG, Murphy JJ, Sreenan JM. Embryo survival in dairy cows managed under pastoral conditions. *Anim Reprod Sci* . 2006;96:297-311.
4. Walker CG, Meier S, Littlejohn MD, Lehnert K, Roche JR, Mitchell MD. Modulation of the maternal immune system by the pre-implantation embryo. *BMC Genomics* . 2010;11:474.
5. Bazer FW, Song G, Thatcher WW. Roles of conceptus secretory proteins in establishment and maintenance of pregnancy in ruminants.*Asian-Aust J Ani Sci* 2012;25(1):1-16.
6. Farin CE, Imakawa K, Roberts RM. In situ localization of mRNA for interferon, ovine trophoblast protein-1, during early embryonic development of the sheep. *Mol Endocrinol.* 1989;3:1099-1107.
7. Uze G, Lutfalla G, Mogensen KE. Alpha and beta interferons and their receptor and their friends and relations. *J Interferon Cytokine Res.* 1995;15:3–26.
8. Parent J, Chapdelaine P, Sirois J, Fortier MA. Expression of microsomal prostaglandin E synthase in bovine endometrium: coexpression with cyclooxygenase type 2 and regulation by interferon-tau. *Endocrinol.* 2002;143:2936–2943.
9. Short EC, Geisert RD, Helmer SD, Zavy MT, Fulton RW. Expression of antiviral activity and induction of 2',5'-oligoadenylate synthetase by conceptus secretory proteins enriched in bovine trophoblast protein-1.*Biol Reprod* . 1991;44:261-268.
10. Schmitt RA, Geisert RD, Zavy MT, Short EC, Blair RM. Uterine Cellular Changes in 2',5'-Oligoadenylate Synthetase during the Bovine Estrous Cycle and Early Pregnancy. *Biol Reprod* . 1993;48:460-466.
11. Johnson GA, Stewart MD, Gray CA, Choi Y, Burghardt RC, Yu-Lee LY, Bazer FW, Spencer TE. Effects of the Estrous Cycle, Pregnancy, and Interferon Tau on 2',5'-Oligoadenylate Synthetase Expression in the Ovine Uterus. *Biol Reprod* . 2001;64:1392-1399.
12. Lengyel P. Tumor-suppressor genes: news about the interferon connection. *Proc Natl Acad Sci U S A* . 1993;90:5893-5895.
13. Salzberg S, Hyman T, Turm H, Kinar Y, Schwartz Y, Nir U, Lejbkowicz F, Huberman E. Ectopic expression of 2-5A synthetase in myeloid cells induces growth arrest and facilitates the appearance of a myeloid differentiation marker. *Cancer Res* . 1997;57:2732-2740.
14. Li XL, Blackford JA, Judge CS, Liu M, Xiao W, Kalvakolanu DV, Hassel BA. RNase-L-dependent destabilization of interferon-induced mRNAs. A role for the 2-5A system in attenuation of the interferon response.*J Biol Chem* . 2000;275:8880-8888.
15. Benech P, Mory Y, Revel M, Chebath J. Structure of two forms of the interferon-induced (2'-5') oligo A synthetase of human cells based on cDNAs and gene sequences. *EMBO J* . 1985;4:2249-2456.
16. Saunders ME, Gewert DR, Tugwell ME, McMahon M, Williams BR. Human 2–5A synthetase: characterization of a novel cDNA and corresponding gene structure. *EMBO J* . 1985;4:1761-1768.
17. Chebath J, Benech P, Hovanessian A, Galabrus J, Revel M. Four different forms of interferon-induced 2'-5' oligo(A) synthetase identified by immunoblotting in human cells. *J Biol Chem* . 1987; 262:3852-3857.

18. Hovanessian AG. Interferon-induced and double-stranded RNA-activated enzymes: a specific protein kinase and 2',5'-oligoadenylate synthetases. *J Interferon Res* . 1991;11:199-205.
19. Marie I, Hovanessian AG. The 69-kDa 2-5A synthetase is composed of two homologous and adjacent functional domains. *J Biol Chem* . 1992;267:9933-9.
20. Hovanessian AG, Laurent AG, Chebath J, Galabru J, Robert N, Svab J. Identification of 69-kd and 100-kd forms of 2-5A synthetase in interferon-treated human cells by specific monoclonal antibodies.*EMBO J* . 1987;6:1273-1280.
21. Marie I, Blanco J, Rebouillat D, Hovanessian AG. 69-kDa and 100-kDa isoforms of interferon-induced (29-59) oligoadenylate synthetase exhibit differential catalytic parameters. *Eur J Biochem* . 1997;248:558-566.
22. Bandyopadhyay S, Ghosh A, Sarkar SN, Sen GC. Production and purification of recombinant 2',5' oligoadenylate synthetase and its mutants using the Baculovirus system. *Biochemistry* . 1998;37:3824-3830.
23. Mirando MA, Short EC Jr, Geisert RD, Vallet JR, Bazer FW. Stimulation of 2',5'-oligoadenylate synthetase activity in sheep endometrium during pregnancy, by intrauterine infusion of ovine trophoblast protein-one, and by intramuscular injection of recombinant bovine interferon-alpha II. *J Reprod Fertil* . 1991;93:599-607.
24. Kashyap K, Jain A, Kasyap S, Verma U, Yadav A, Dubey A, Sori S. Genetic resources on goat in India: A review. *Int J Fauna Biol Stud.* 2020;7(2):27-33.
25. Islam MM, Shabana A, Modi RJ, Wadhwani KN. Scenario of livestock and poultry in India and their contribution to national economy. *Int J Sci Env Tech.* 2016;5(3):956-965.
26. Singh NS, Gawande PG, Mishra OP, Nema RK, Mishra UK, Singh M. Accuracy of ultrasonograph in early pregnancy diagnosis in does.*Asian-Aust J Anim Sci* . 2004;17(6):760-768.
27. Jain T, Jain T, Chandrakar K, Tripathi SM, Mukherjee K, Shakya S, Tiwari SK, Mishra OP. Cathepsin L gene: Molecular characterization, functional analysis and expression profile in the endometrium of goat (Capra hircus). *Animal Gene* . 2021;200116.
28. Gill SC, von Hippel PH. Calculation of protein extinction coefficients from amino acid sequence data. *Anal Biochem* . 1989;182:319-326.
29. Bachmair A, Finley D, Varshavsky A. In vivo half-life of a protein is a function of its amino-terminal residue. *Science* . 1986;234:179-186.
30. Guruprasad K, Reddy BVB, Pandit MW. Correlation between stability of a protein and its dipeptide composition: a novel approach for predicting in vivo stability of a protein from its primary sequence.*Protein Eng.* 1990;4:155-161.
31. Ikai AJ. Thermostability and aliphatic index of globular proteins.*J Biochem.* 1980;88:1895-1898.
32. Kyte J, Doolittle RF. A simple method for displaying the hydropathic character of a protein. *J Mol Biol.* 1982;157:105-132.
33. Almagro AJJ, Tsirigos KD, Sønderby CK *et al.* SignalP 5.0 improves signal peptide predictions using deep neural networks. *Nat Biotechnol.* 2019;37:420–423.
34. Krogh A, Larsson B, von Heijne G, Sonnhammer EL. Predicting transmembrane protein topology with a hidden Markov model: application to complete genomes. *J Mol Biol.* 2001;305(3):567-580.
35. Geourjon C, Deléage G. SOPMA: significant improvements in protein secondary structure prediction by consensus prediction from multiple alignments. *Comput Appl Biosci.* 1995;11(6):681-684.
36. Klausen MS, Jespersen MC, Nielsen H, Jensen KK, Jurtz VI, Sønderby CK, Sommer MOA, Winther O, Nielsen M, Petersen B, Marcatili P. NetSurfP-2.0: Improved prediction of protein structural features by integrated deep learning. Proteins: Struct *Funct Bioinf.* 2019;87(6):520-527.
37. Geertz-Hansen HM, Blom N, Feist A, Brunak S, Petersen TH. Cofactory: A sequence-based prediction method of cofactor specificity of Rossmann folds. *Proteins* . 2014;82(9):1819-28.
38. Olsen TH, Yesiltas B, Marin FI, Pertseva M, García-Moreno PJ, Gregersen S, Overgaard MT, Jacobsen C, Lund O, Hansen EB, Marcatili P. AnOxPePred: Using deep learning for the prediction of antioxidative properties of peptides. *Sci Rep* . 2020;10:21471.
39. Julenius K. NetCGlyc 1.0: Prediction of mammalian C-mannosylation sites. Glycobiology. 2007;17:868-

876.
40. Kiemer L, Bendtsen JD, Blom N. NetAcet: Prediction of N-terminal acetylation sites. Bioinformatics. 2005;21:1269-1270.
41. Gíslason MH, Nielsen H, Armenteros JJA, Johansen AR. Prediction of GPI-anchored proteins with pointer neural networks. *Curr Res Biotechnol.* 2021;3:6-13.
42. Steentoft C, Vakhrushev SY, Joshi HJ, Kong Y, Vester-Christensen MB, Schjoldager KT, Lavrsen K, Dabelsteen S, Pedersen NB, Marcos-Silva L, Gupta R, Bennett EP, Mandel U, Brunak S, Wandall HH, Levery SB, Clausen H. Precision mapping of the human O-GalNAc glycoproteome through simple cell technology. *EMBO J* . 2013;32(10):1478-88.
43. Johansen MB, Kiemer L, Brunak S. Analysis and prediction of mammalian protein glycation. Glycobiology. 2006;16(9):844-853.
44. Blom N, Gammeltoft S, Brunak S. Sequence- and structure-based prediction of eukaryotic protein phosphorylation sites. J Mol Biol. 1999;294:1351-1362.
45. Duckert P, Brunak S, Blom N. Prediction of proprotein convertase cleavage sites. *Protein Eng Des Sel* . 2004;17:107-112.
46. Li A, Xue Y, Jin C, Wang M, Yao X. Prediction of Nepsilon-acetylation on internal lysines implemented in Bayesian Discriminant Method. Biochem Biophys Res Commun. 2006;350(4):818-824.
47. Zhao Q, Xie Y, Zheng Y, Jiang S, Liu W, Mu W, Zhao Y, Xue Y, Ren J. GPS-SUMO: a tool for the prediction of sumoylation sites and SUMO-interaction motifs**.** *Nucleic Acids Res* **.**2014;42(W1):W325-W330.
48. Webb B, Sali A. Comparative Protein Structure Modeling Using Modeller.*Current Protocols in Bioinformatics* . 2016:5.6.1-5.6.37.
49. Waterhouse A, Bertoni M, Bienert S, Studer G, Tauriello G, Gumienny R, Heer FT, de Beer TAP, Rempfer C, Bordoli L, Lepore R, Schwede T. SWISS-MODEL: homology modelling of protein structures and complexes.*Nucleic Acids Res* . 2018;46:W296-W303.
50. Kelley LA, Mezulis S, Yates CM, Wass MN, Sternberg MJE. The Phyre2 web portal for protein modeling, prediction and analysis. *Nature Protocols* . 2015;10:845-858.
51. Combet C, Jambon M, Deléage G, Geourjon C. Geno3D: automatic comparative molecular modelling of protein. *Bioinformatics* . 2002;18(1):213-4. doi:10.1093
52. Colovos C, Yeates TO. Verification of protein structures: patterns of nonbonded atomic interactions. *Protein Sci* . 1993;2(9):1511-9. doi:10.1002/pro.5560020916
53. Laskowski RA, MacArthur MW, Moss DS, Thornton JM. PROCHECK - a program to check the stereochemical quality of protein structures. *J App Cryst* . 1993;26:283-291.
54. Eisenberg D, Lüthy R, Bowie JU. VERIFY3D: assessment of protein models with three-dimensional profiles. *Methods Enzymol* . 1997;277:396-404.
55. Ramachandran GN, Ramakrishnan C, Sasisekharan V. Stereochemistry of polypeptide chain configurations. *J Mol Biol* . 1963;7:95-99.
56. Pettersen EF, Goddard TD, Huang CC, Couch GS, Greenblatt DM, Meng EC, Ferrin TE. UCSF Chimera-A visualization system for exploratory research and analysis. *J Comput Chem* . 2004;25:1605-1612.
57. Letunic I, Bork P. 20 years of the SMART protein domain annotation resource. *Nucleic Acids Res* . 2018;4:46(D1):D493-D496.
58. Chandrakar K, Jain A, Khan JR, Jain T, Singh M, Mishra OP. Molecular characterization and expression profile of interferon stimulated gene 15 (ISG15) in the endometrium of Goat. *Theriogenol.* 202;142, 348-354.
59. Livak KJ, Schmittgen TD. Analysis of relative gene expression data using real time quantitative PCR and the 2 Delta Delta C(T) method.*Methods* . 2001;25:402–408.
60. Rios JJ, Perelygin AA, Long MT, Lear TL, Zharkikh AA *et al* . Characterization of the equine 2'-5' oligoadenylate synthetase 1 (OAS1) and ribonuclease L (RNASEL) innate immunity genes, *BMC Genomics* . 2007;7(8):313.
61. Eskildsen S, Justesen J, Schierup M H & Hartmann R, Characterization of the 2'-5'-oligoadenylate

synthetase ubiquitin-like family.*Nucleic Acids Res* . 2003;31:3166-3173.
62. Batra K, Nanda T, Kumar A, Kumari R, Kumar V, Maan S. Molecular characterization of OAS1 as a biomarker molecule for early pregnancy diagnosis in *Bubalus bubalis. Indian J Biotechnol.* 2019;19:97-107.
63. Dubchak I, Muchnik I, Mayor C, Dralyuk I, Kim SH. Recognition of a protein fold in the context of the Structural Classification of Proteins (SCOP) classification. *Proteins* . 1999;35:401-407.
64. Cai CZ, Han LY, Ji ZL, Chen X, Chen YZ. SVM-Prot: Web-based support vector machine software for functional classification of a protein from its primary sequence. *Nucleic Acids Res* . 2003;31:3692-3697.
65. Bock JR, Gough DA. Whole-proteome interaction mining.*Bioinformatics* . 2003;19:125-134.
66. Chou KC, Cai YD. Prediction of protein subcellular locations by GO-FunD-PseAA predictor. *Biochem Biophys Res Commun* . 2004;320:1236-1239.
67. Schneider G, Wrede P. The rational design of amino acid sequences by artificial neural networks and simulated molecular evolution: de novo design of an idealized leader peptidase cleavage site. *Biophys J* . 1994;66:335-344.
68. Brown MP, Grundy WN, Lin D, Cristianini N, Sugnet CW, et al. Knowledge-based analysis of microarray gene expression data by using support vector machines. *Proc Natl Acad Sci U S A* . 2000;97:262-267.
69. Ward JJ, McGuffin LJ, Buxton BF, Jones DT. Secondary structure prediction with support vector machines. *Bioinformatics.*2003;19:1650-1655.
70. Shen HB, Yang J, Chou KC. Fuzzy KNN for predicting membrane protein types from pseudo-amino acid composition. *J Theor Biol* . 2006;240(1):9-13.
71. Chou KC, Shen HB. MemType-2L: a web server for predicting membrane proteins and their types by incorporating evolution information through Pse-PSSM. *Biochem Biophys Res Commun* . 2007;360(2):339-345.
72. Besse S, Rebouillat D, Marie I, Puvion-Dutilleul F, Hovanessian AG. Ultrastructural localization of interferon-inducible double-stranded RNA-activated enzymes in human cells. *Exp Cell Res* . 1998;239(2):379-392.
73. Kjaer KH, Pahus J, Hansen MF, et al. Mitochondrial localization of the OAS1 p46 isoform associated with a common single nucleotide polymorphism. *BMC Cell Biol* . 2014;15:33.
74. Breda A, Valadares N F, Norberto de Souza O & Garratt R C, Protein Structure, Modelling and Applications, 2006 May 1 [Updated 2007 Sep 14]. In: Gruber A, Durham AM, Huynh C, *et al* , editors. Bioinformatics in Tropical Disease. Research: A Practical and Case-Study Approach [Internet]. Bethesda (MD): National Center for Biotechnology Information (US) 2008. Chapter A06.
75. Momen-Roknabadi A, Sadeghi M, Pezeshk H, Marashi SA. Impact of residue accessible surface area on the prediction of protein secondary structures. *BMC Bioinformatics* . 2008;9: 357.
76. Ali S, Hassan MD, Islam A, Ahmad F. A review of methods available to estimate solvent-accessible surface areas of soluble proteins in the folded and unfolded states. *Curr Protein Pept Sci* . 2014;15:456-476.
77. Singh RR. The potential use of peptides and vaccination to treat systemic lupus erythematosus. *Curr Opin Rheumatol* . 2000;12:399-406.
78. Haselden BM, Kay AB, Larche M. Peptide-mediated immune responses in specific immunotherapy. *Int Arch Allergy Immunol* . 2000;122:229-37.
79. Tong JC, Tan TW, Ranganathan S. Methods and protocols for prediction of immunogenic epitopes. *Briefings in Bioinformatics* . 2007;8(2):96-108.
80. Roy J. Posttranslational modifications and the immunogenicity of biotherapeutics. *J Immunol Res.* 2016*;* 15.
81. Jayaprakash NG, Surolia A. Role of glycosylation in nucleating protein folding and stability. *Biochem J* . 2017;474:2333-2347.
82. Hanisch FG. O-glycosylation of the mucin type. *Biol Chem* . 2001;382(2):143-9.
83. Liu Y, Gu W, Zhang W, Wang J. Predict and Analyze Protein Glycation Sites with the mRMR and IFS Methods. *Biomed Res Int* . 2015;12:1-6.
84. Ardito F, Giuliani M, Perrone D, Troiano G, Muzio LL. The crucial role of protein phosphorylation in

cell signaling and its use as targeted therapy (Review). *Int J Mol Med* . 2017;40(2):271-280.
85. Faiola F, Liu X, Lo S, Pan S, Zhang K, Lymar E, Farina A, Martinez E. Dual regulation of c-Myc by p300 via acetylation-dependent control of Myc protein turnover and coactivation of Myc-induced transcription. Mol Cell Biol. 2005 Dec;25(23):10220-34.
86. Brunet A, Sweeney LB, Sturgill JF, Chua KF, Greer PL, Lin Y, Tran H, Ross SE, Mostoslavsky R, Cohen HY, Hu LS, Cheng HL, Jedrychowski MP, Gygi SP, Sinclair DA, Alt FW, Greenberg ME. Stress-dependent regulation of FOXO transcription factors by the SIRT1 deacetylase. Science. 2004 Mar 26;303(5666):2011-5.
87. Murr R, Loizou JI, Yang YG, et al. Histone acetylation by Trrap-Tip60 modulates loading of repair proteins and repair of DNA double-strand breaks. *Nat Cell Biol.* 2006;8:91–99.
88. Subramanian C, Opipari AW Jr, Bian X, Castle VP, Kwok RP. Ku70 acetylation mediates neuroblastoma cell death induced by histone deacetylase inhibitors. *Proc Natl Acad Sci U S A*.2005;102(13):4842-4847.
89. Cohen HY, Lavu S, Bitterman KJ, Hekking B, Imahiyerobo TA, Miller C, Frye R, Ploegh H, Kessler BM, Sinclair DA. Acetylation of the C terminus of Ku70 by CBP and PCAF controls Bax-mediated apoptosis.*Mol Cell* . 2004;13(5):627-638.
90. Yuan ZL, Guan YJ, Chatterjee D, Chin YE. Stat3 dimerization regulated by reversible acetylation of a single lysine residue. *Science* . 2005;307(5707):269-273.
91. Bannister AJ, Miska EA, Gorlich D, Kouzarides T. Acetylation of importin-alpha nuclear import factors by CBP/p300. *Curr Biol* . 2000;10(8):467-470.
92. Han ZJ, Feng YH, Gu BH, Li YM, Chen H. The post-translational modification, SUMOylation, and cancer (Review). *Int J Oncol* . 2018;52:1081-1094.
93. Wiedemann C, Kumar A, Lang A, Ohlenschlager O. Cysteines and Disulfide Bonds as Structure-Forming Units: Insights from Different Domains of Life and the Potential for Characterization by NMR. *Front Chem* . 2020;8:280.
94. Zhang Y. Protein Structure Prediction: Is It Useful? *Curr Opin Struct Biol* . 2009;19(2):145-155.
95. Joshi I, Kumar S, Kaur A, Mukhopadhyay C S, Kumar D. Homology modeling of buffalo (*Bubalus bubalis*) interferon- tau protein, *Am J Bioinform.* 2012;1:79-86.
96. Dawson N, Sillitoe I, Marsden RL, Orengo CA. The classification of protein domains. Bioinformatics. *Springer.* 2017;137-164 p.
97. Wang Y, Zhang H, Zhong H, Xue Z. Protein domain identification methods and online resources. *Comput Struct Biotechnol J* . 2021;19:1145-1153.
98. Hartmann R, Justesen J, Sarkar SN, Sen GC, Yee VC. Crystal structure of the 2'-specific and double-stranded RNA-activated interferon-induced antiviral protein 2'-5'-oligoadenylate synthetase.*Mol Cell* . 2003;12:1173-1185.
99. Ghosh SK, Kusari J, Bandyopadhyay SK, Samanta H, Kumar R, Sen GC. Cloning, sequencing, and expression of two murine 2'-5'-oligoadenylate synthetases. Structure-function relationships. *J Biol Chem* . 1991;266(23):15293-15299.
100. Hovanessian AG, Justesen J. The human 2'-5'oligoadenylate synthetase family: unique interferon-inducible enzymes catalyzing 2'-5' instead of 3'-5' phosphodiester bond formation. *Biochimie* . 2007;89:779-88.
101. Kumar M, Gouw M, Michael S, Samano-Sanchez H, Pancsa R, Glavina J, Diakogianni A, Valverde JA, Bukirova D, Čalyševa J, Palopoli N, Davey NE, Chemes LB, Gibson TJ. ELM-the eukaryotic linear motif resource in 2020. *Nucleic Acids Res. 2020;* 48(D1):D296-D306.
102. Dinkel H, Van Roey K, Michael S, Kumar M, Uyar B, Altenberg B, Milchevskaya V, Schneider M, Kühn H, Behrendt A, Dahl SL, Damerell V, Diebel S, Kalman S, Klein S, Knudsen AC, Mäder C, Merrill S, Staudt A, Thiel V, Welti L, Davey NE, Diella F, Gibson TJ. ELM 2016–data update and new functionality of the eukaryotic linear motif resource.*Nucleic Acids Res* . 2016;44(D1):D294-300.
103. Szklarczyk D, Gable AL, Lyon D, Junge A, Wyder S, Huerta-Cepas J, Simonovic M, Doncheva NT, Morris JH, Bork P, Jensen LJ, Mering CV. STRING v11: protein-protein association networks with increased coverage, supporting functional discovery in genome-wide experimental datasets. *Nucleic*

Acids Res . 2019;47(D1):D607-D613.
104. Barros CM, Plante C, Thatcher WW, Hansen PJ. Regulation of bovine endometrial secretion of prostaglandins and synthesis of 2',5'-oligoadenylate synthetase interferon-a molecules. *Am J Reprod Immunol* . 1991; 25:146-152.
105. Bazer FW, Spencer TE, Johnson GA. Interferons and uterine receptivity.*Semin Reprod Med* . 2009;27:90-102.
106. Bazer, FW, Spencer T E, Johnson GA, Burghardt RC. Uterine receptivity to implantation of blastocysts in mammals. *Front. Biosci* . 2011; S3:745-767.
107. Farin CE, Imakawa K, Hansen TR, McDonnell J J, Murphy CN. Expression of trophoblastic interferon genes in sheep and cattle. *Biol Reprod.* 1990;43:210-218.
108. Kumar S, Mitnik C, Valente G, Smith F. Expansion and molecular evolution of the interferon-induced 2'-5' oligoadenylate synthetase gene family. *Mol Biol Evol* . 2000;17:738-750.
109. Spencer TE, Ott TL, Bazer FW. Tau interferon: pregnancy recognition signal in ruminants. *Proc Soc Exp Biol Med.* 1996;213:215–229.
110. Martal JL, Chene NM, Huynh LP, L'Haridon RM, Reinaud PB, Guillomot MW, Charlier MA, Charpigny SY. IFN-tau: a novel subtype I IFN1. Structural characteristics, non-ubiquitous expression, structurefunction relationships, a pregnancy hormonal embryonic signal and cross-species therapeutic potentialities. *Biochimie* . 1998;80:755–777.

LEGENDS OF FIGURES

FIGURE 1 Multiple alignment of the deduced amino acid sequence of cpOAS1 protein with that of different species.

FIGURE 2 Phylogram showing the evolutionary relationship among the cDNA sequences of the OAS1 gene of different species by using the MegAlign software. It revealed three distinct clades, clade A includes large ruminant species, clade B includes small ruminant species and clade C includes non-ruminant species.

FIGURE 3 Hydrophilicity analysis of the cpOAS1 protein by ProtScale indicates many hydrophilic amino acids are present in the protein.

FIGURE 4 Multilocalization of cpOAS1 protein by PSORT II (4a) and DeepLoc-1.0 servers (4b)

FIGURE 5 Combination of buried and exposed amino acid residues, RSA and disorders in the cpOAS1 protein

FIGURE 6 Prediction of mucin-type GalNAc O-glycosylation (6A) and Glycation (6B) sites at amino groups of a lysine residue in the cpOAS1 protein.

FIGURE 7 Prediction of 3-D structure of cpOAS1 protein generated from MODELLER 9.18 (P1), SWISS-MODEL (P2), PHYRE 2 (P3) and GENO3D (P4).

FIGURE 8A Ramachandran plot generated from SWISS-MODEL (P2). It shows 94.6 % residues in the most favoured region and 5.4 % additional allowed regions (%) and none in the disallowed region.

FIGURE 8B Superimposition of SWISS-MODEL (P2) model and porcine (4rwp) generated in UCSF Chimera

FIGURE 9 Prediction of 51 different types of eukaryotic linear motifs and 120 instances in the cpOAS1 protein.

FIGURE 10 Prediction of the interaction of cpOAS1 protein with top ten proteins by STRING 11.0 tool.

FIGURE 11 Relative quantitative PCR analysis of cpOAS1 mRNA in the endometrial tissue of pregnant (P) and cyclic does. Bars indicate mean ± SEM values (n = 6). Different letters indicate significant difference ($P < 0.05$).

FIGURE 12 Detection of OAS protein by western blotting. Detection of OAS protein on PVDF membrane (A) and relative expression of OAS protein (B) in the endometrial tissue of pregnant and non-pregnant does.

M: Molecular weight markers (Himedia); Lanes 1: Non-pregnant doe; Lanes 2: 16 to 24 days pregnant doe; Lane 3: 25 to 40 days pregnant doe. Bars indicate mean ± SEM values (n = 6). Different alphabets indicate significant difference ($P < 0.05$).

LEGENDS OF TABLES

TABLE 1 List of primers used for cpOAS1 amplification and qPCR

TABLE 2 Various physical and chemical parameters of cpOAS1 protein

TABLE 3(a) Different locations of cpOAS1 protein by DeepLoc-1.0 servers

TABLE 3(b) Different locations of cpOAS1 protein by PSORT II

TABLE 4 List of sequences that shows the anti-oxidative properties in the cpOAS1

TABLE 5A Prediction of B cell epitopes using IEDB analysis

TABLE 5B Prediction of T cell epitopes using IEDB analysis

TABLE 6 Prediction of different phosphorylation sites

TABLE 7 Prediction of different internal acetylation sites in the cpOAS1 protein sequence

TABLE 8 Different predicted Sumoylation sites in the cpOAS1

TABLE 9 Validation properties of different models

TABLE 10 Domains obtained from different database

TABLE 11 Top ten proteins that interact with cpOAS1 protein as predicted by STRING

TABLE 12 Different metal binding, active and NTP sites in the cpOAS1 protein

Hosted file

`Jain, A et al_2022_cpOAS1_Tables.docx` available at https://authorea.com/users/494756/articles/576729-2-5-oligoadenylate-synthetase1-oas1-molecular-structural-integrative-bioinformatics-and-functional-analysis-in-the-endometrium-of-goat-capra-hircus

Jain, A et al_2022_FIGURE 1

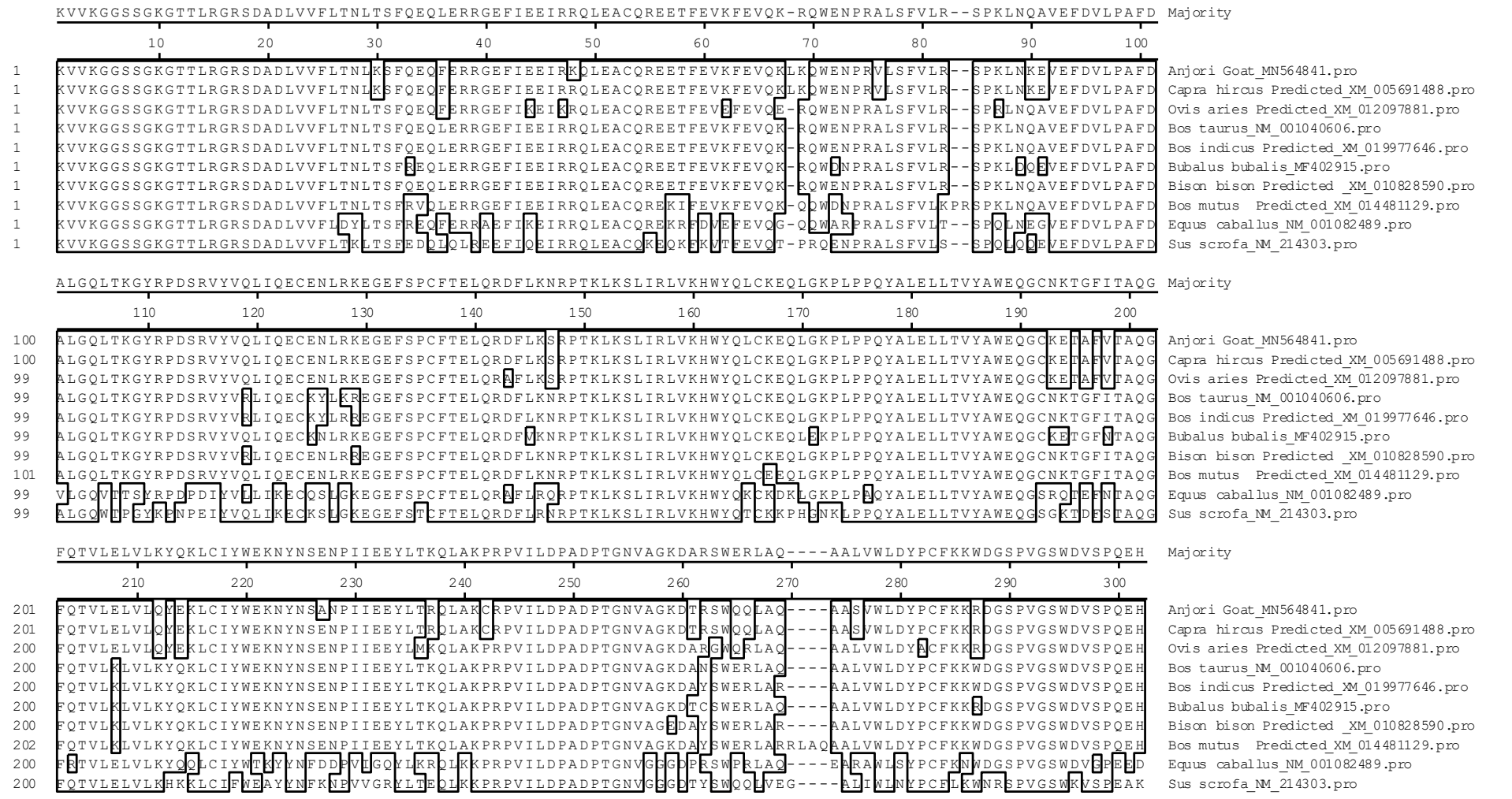

Jain, A et al_2022_FIGURE 2

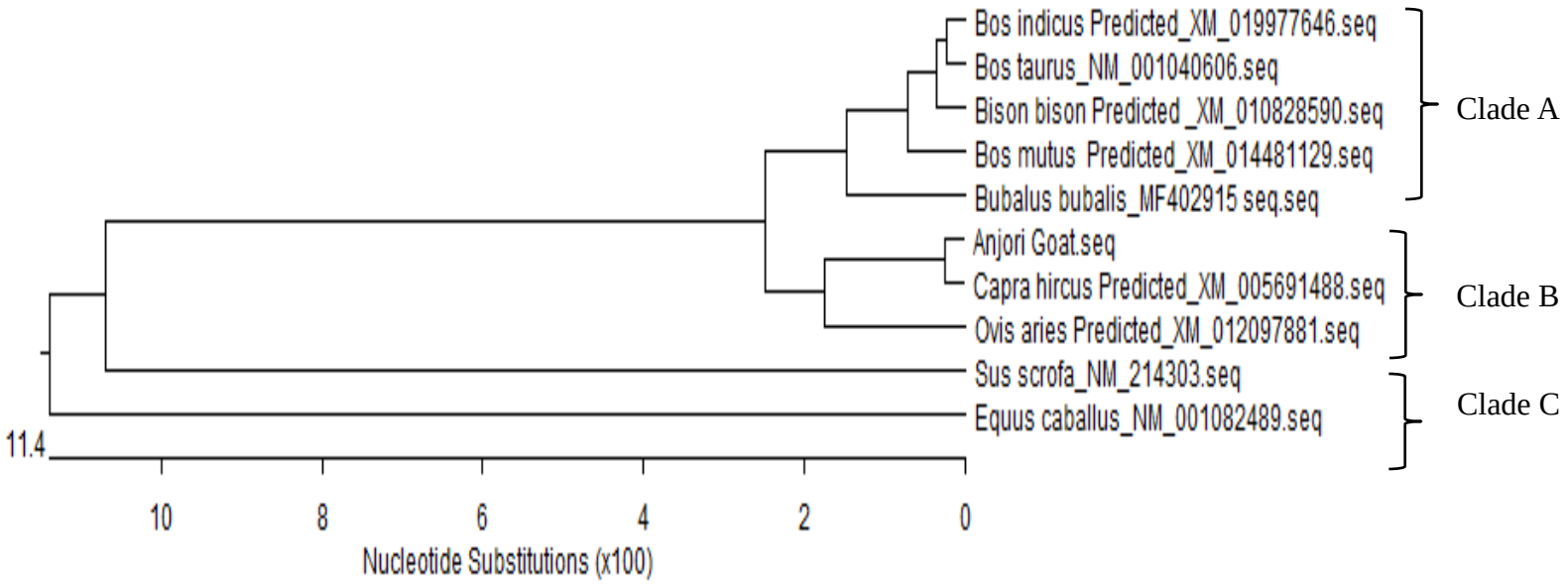

Jain, A et al_2022_FIGURE 3

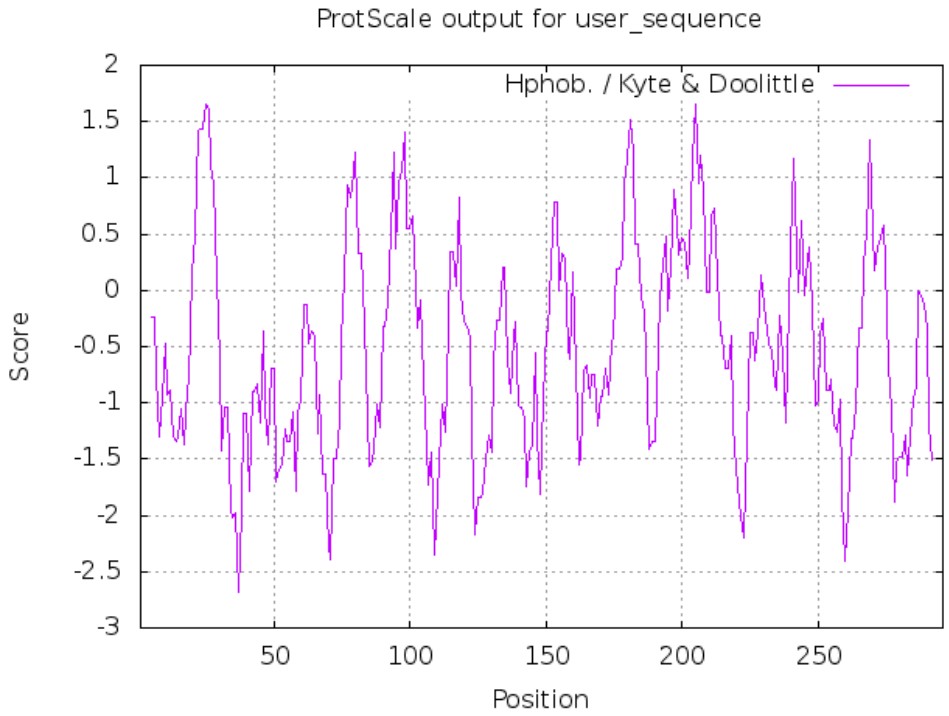

Jain, A et al_2022_FIGURE 4

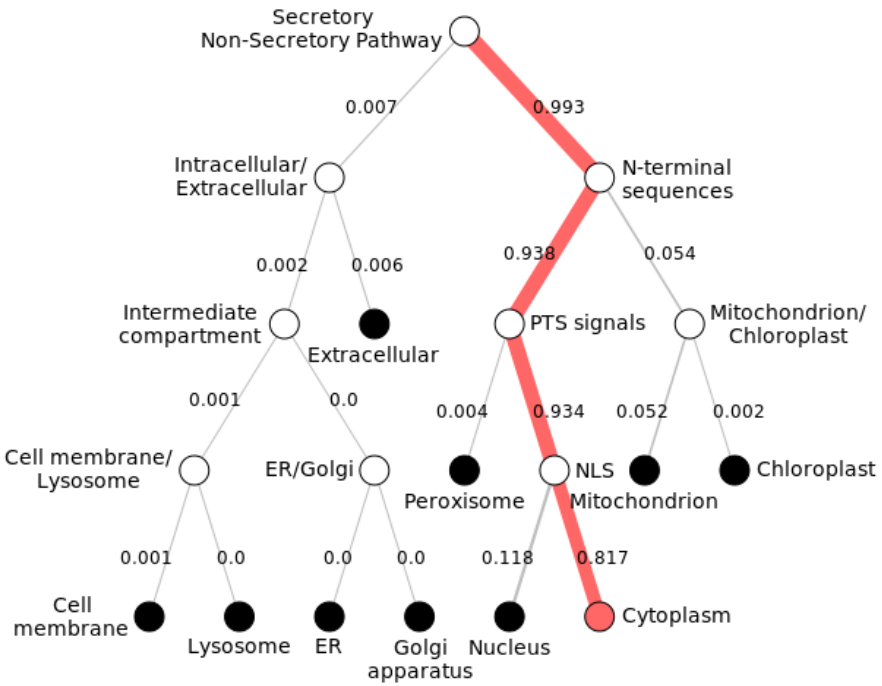

Jain, A et al_2022_FIGURE 5

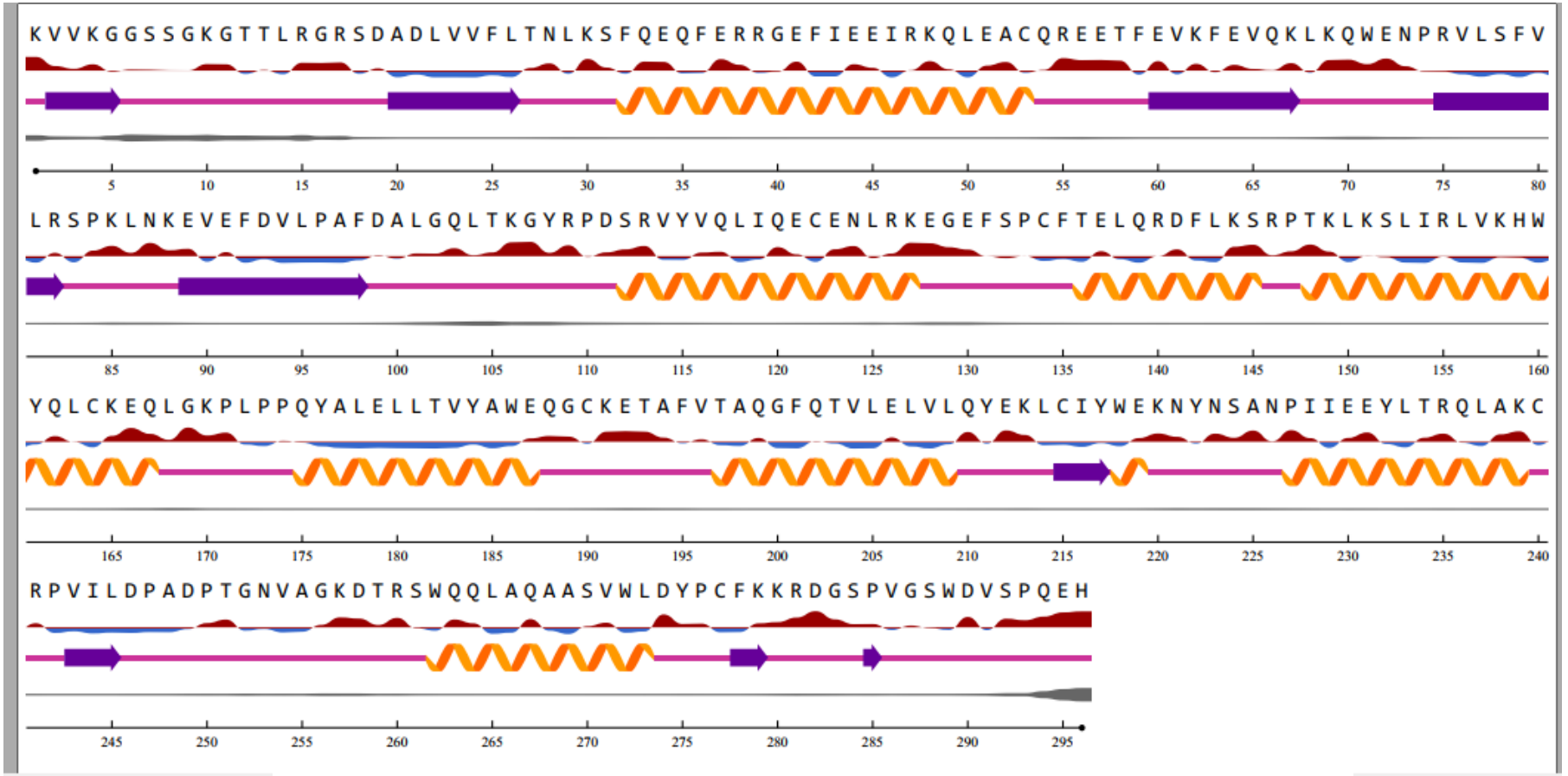

Relative Surface Accessibility: Red is exposed and blue is buried, thresholded at 25%.
Secondary Structure: Helix, Strand, Coil.
Disorder: Thickness of line equals probability of disordered residue.

Jain, A et al_2022_FIGURE 6

```
##gff-version 2
##source-version NetOGlyc 4.0.0.13
##date 21-6-20
##Type Protein
#seqname        source  feature start   end     score   strand  frame   comment
SEQUENCE        netOGlyc-4.0.0.13       CARBOHYD        7       7       0.436424        .       .
SEQUENCE        netOGlyc-4.0.0.13       CARBOHYD        8       8       0.509214        .       .       #POSITIVE
SEQUENCE        netOGlyc-4.0.0.13       CARBOHYD        12      12      0.135737        .       .
SEQUENCE        netOGlyc-4.0.0.13       CARBOHYD        13      13      0.290014        .       .
SEQUENCE        netOGlyc-4.0.0.13       CARBOHYD        18      18      0.109704        .       .
SEQUENCE        netOGlyc-4.0.0.13       CARBOHYD        27      27      0.0260361       .       .
SEQUENCE        netOGlyc-4.0.0.13       CARBOHYD        31      31      0.0268332       .       .
SEQUENCE        netOGlyc-4.0.0.13       CARBOHYD        58      58      0.0476946       .       .
SEQUENCE        netOGlyc-4.0.0.13       CARBOHYD        78      78      0.0128988       .       .
SEQUENCE        netOGlyc-4.0.0.13       CARBOHYD        83      83      0.023187        .       .
SEQUENCE        netOGlyc-4.0.0.13       CARBOHYD        105     105     0.0543519       .       .
SEQUENCE        netOGlyc-4.0.0.13       CARBOHYD        112     112     0.364614        .       .
SEQUENCE        netOGlyc-4.0.0.13       CARBOHYD        132     132     0.109839        .       .
SEQUENCE        netOGlyc-4.0.0.13       CARBOHYD        136     136     0.0903724       .       .
SEQUENCE        netOGlyc-4.0.0.13       CARBOHYD        145     145     0.217948        .       .
SEQUENCE        netOGlyc-4.0.0.13       CARBOHYD        148     148     0.139305        .       .
SEQUENCE        netOGlyc-4.0.0.13       CARBOHYD        152     152     0.189613        .       .
SEQUENCE        netOGlyc-4.0.0.13       CARBOHYD        182     182     0.0870225       .       .
SEQUENCE        netOGlyc-4.0.0.13       CARBOHYD        193     193     0.0485995       .       .
SEQUENCE        netOGlyc-4.0.0.13       CARBOHYD        197     197     0.184416        .       .
SEQUENCE        netOGlyc-4.0.0.13       CARBOHYD        203     203     0.0630673       .       .
SEQUENCE        netOGlyc-4.0.0.13       CARBOHYD        224     224     0.118056        .       .
SEQUENCE        netOGlyc-4.0.0.13       CARBOHYD        234     234     0.139841        .       .
SEQUENCE        netOGlyc-4.0.0.13       CARBOHYD        251     251     0.538327        .       .       #POSITIVE
SEQUENCE        netOGlyc-4.0.0.13       CARBOHYD        259     259     0.227847        .       .
SEQUENCE        netOGlyc-4.0.0.13       CARBOHYD        261     261     0.134803        .       .
SEQUENCE        netOGlyc-4.0.0.13       CARBOHYD        270     270     0.26259 .       .
SEQUENCE        netOGlyc-4.0.0.13       CARBOHYD        284     284     0.271729        .       .
SEQUENCE        netOGlyc-4.0.0.13       CARBOHYD        288     288     0.29626 .       .
SEQUENCE        netOGlyc-4.0.0.13       CARBOHYD        292     292     0.316098        .       .
```

6A

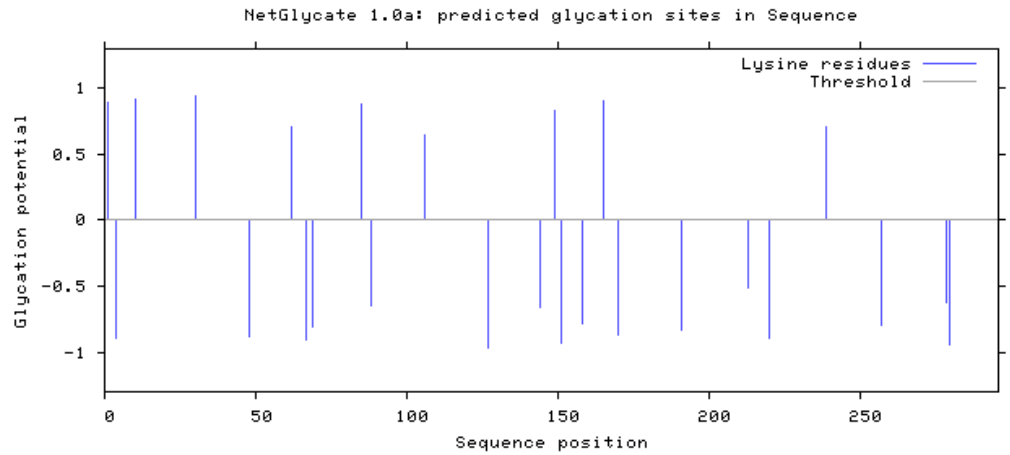

6B

Jain et al_2022_FIGURE 7

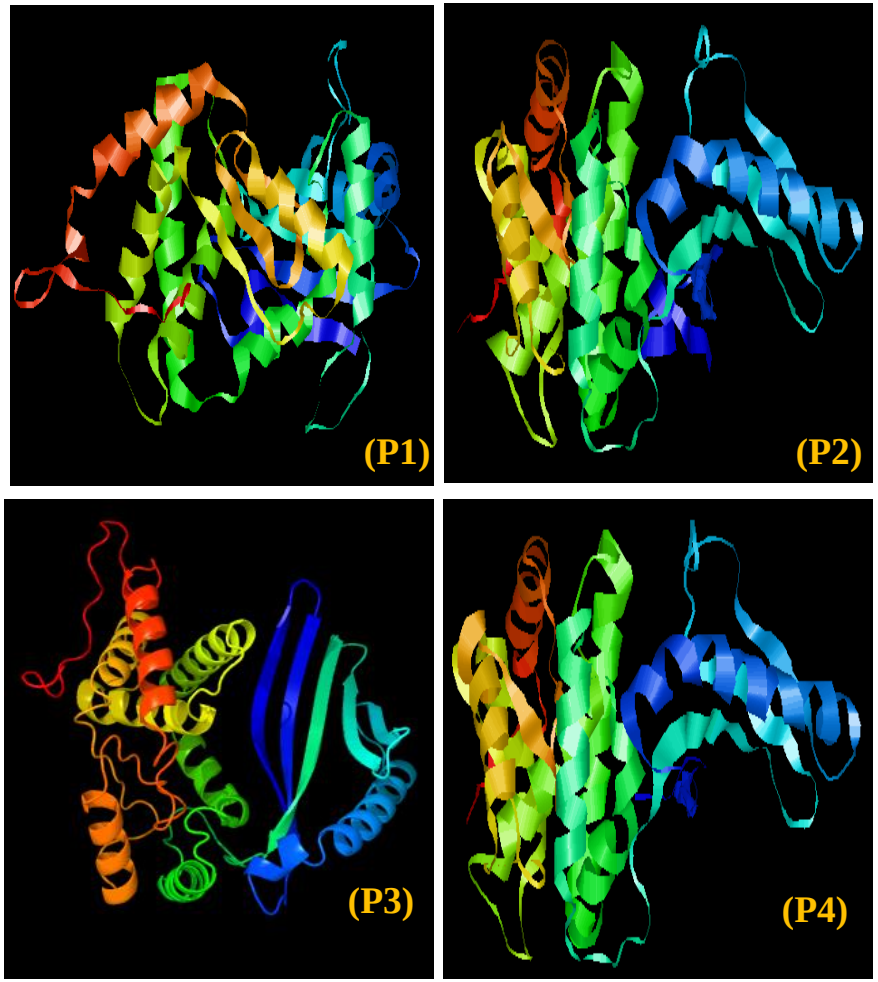

Jain, A et al_2022_FIGURE 8(A)

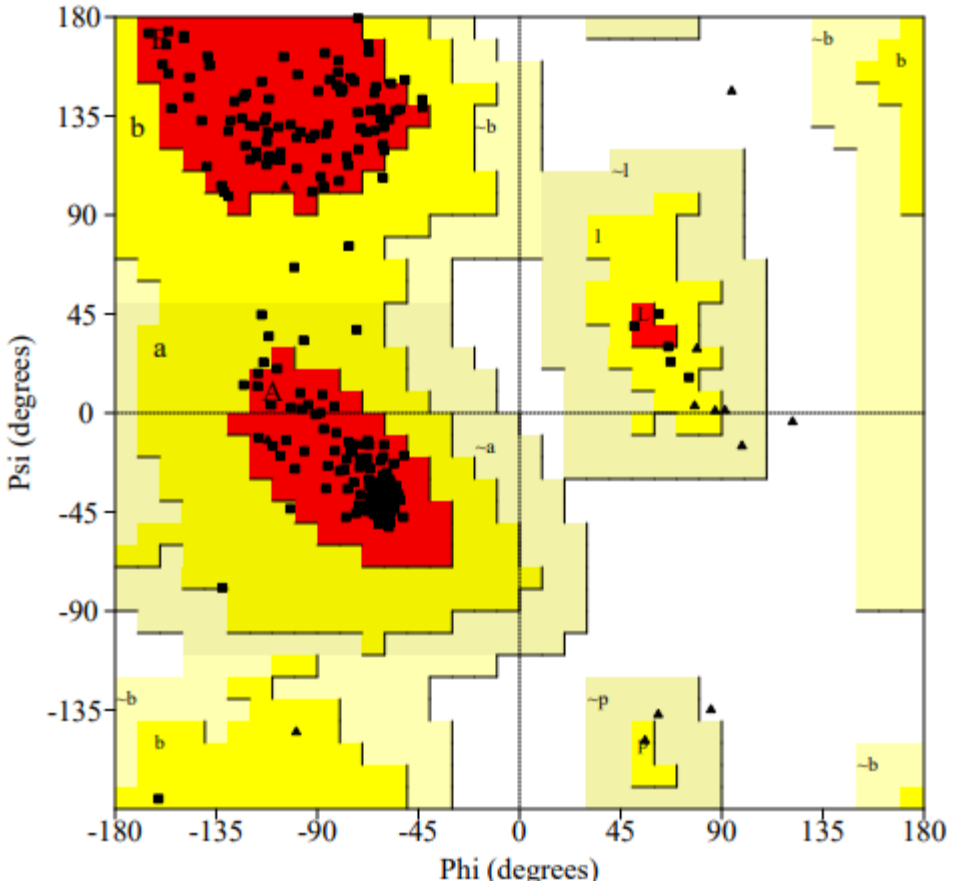

Jain, A et al_2022_FIGURE 8(B)

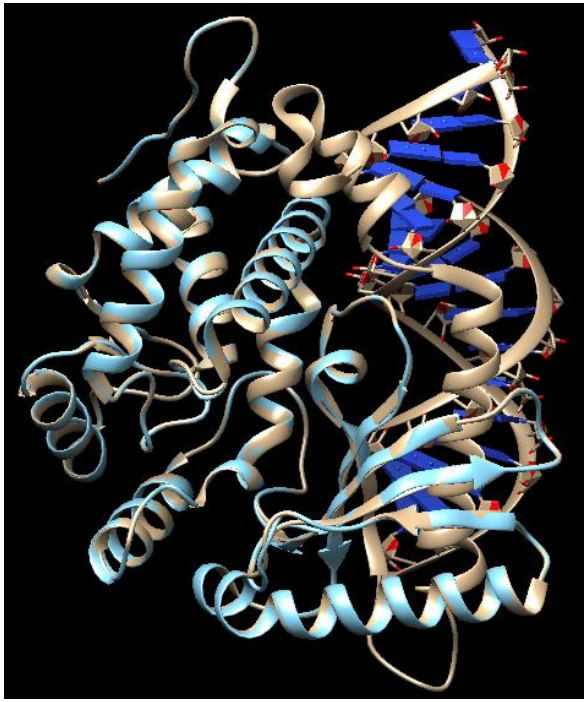

Jain, A et al_2022_FIGURE 9

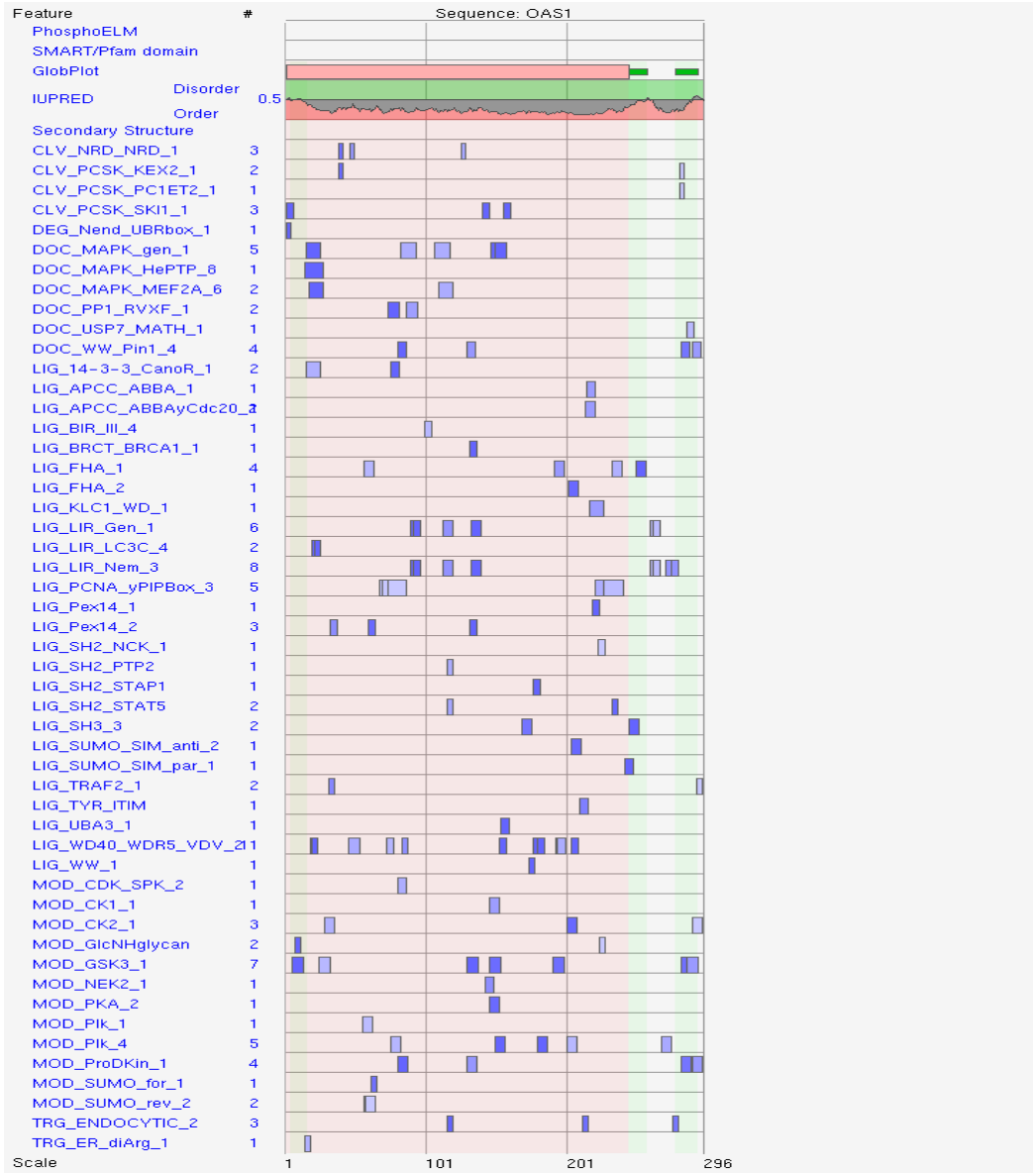

Jain, A et al_2022_FIGURE 10

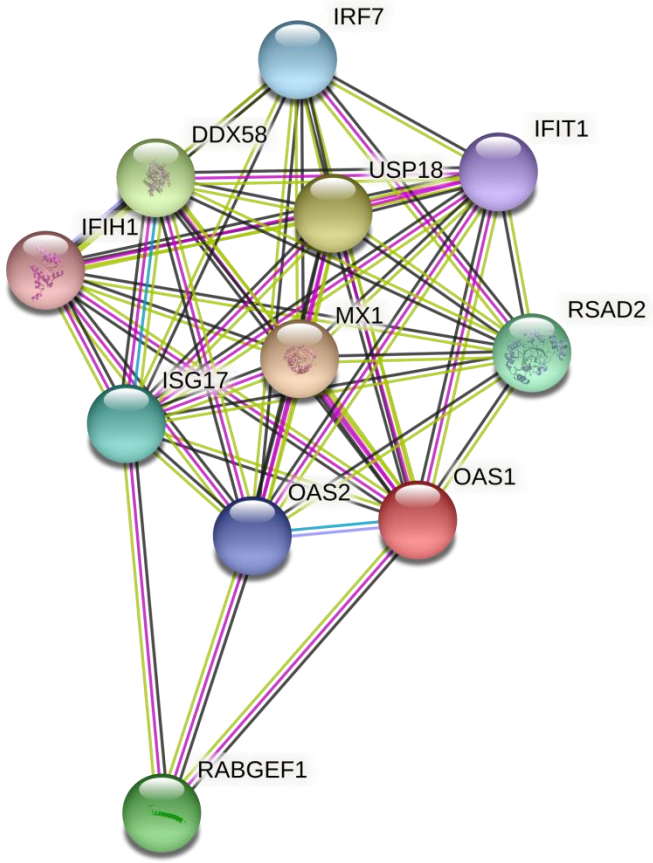

Jain, A et al_2022_FIGURE 11

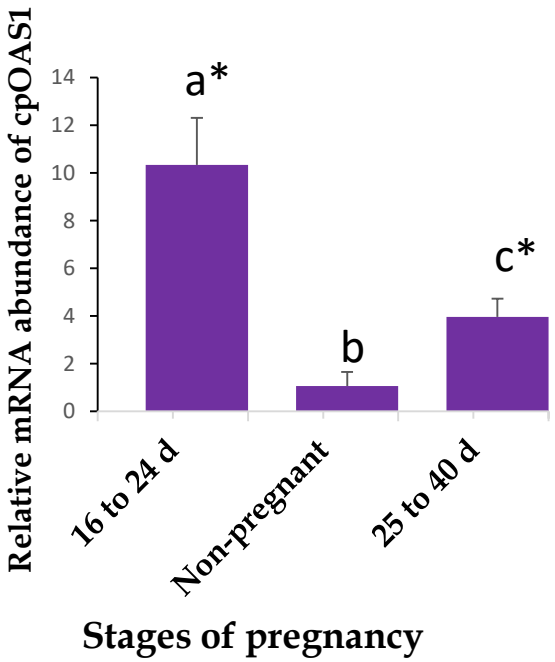

Jain, A et al_2022_FIGURE 12

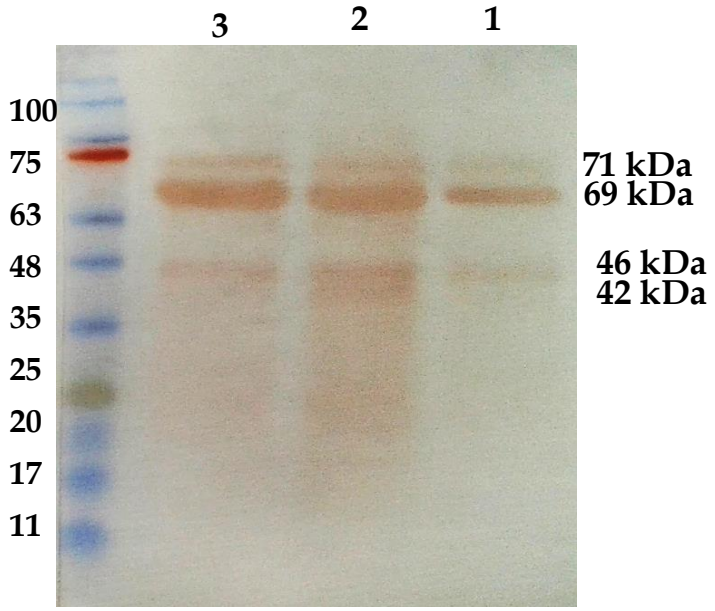

15A

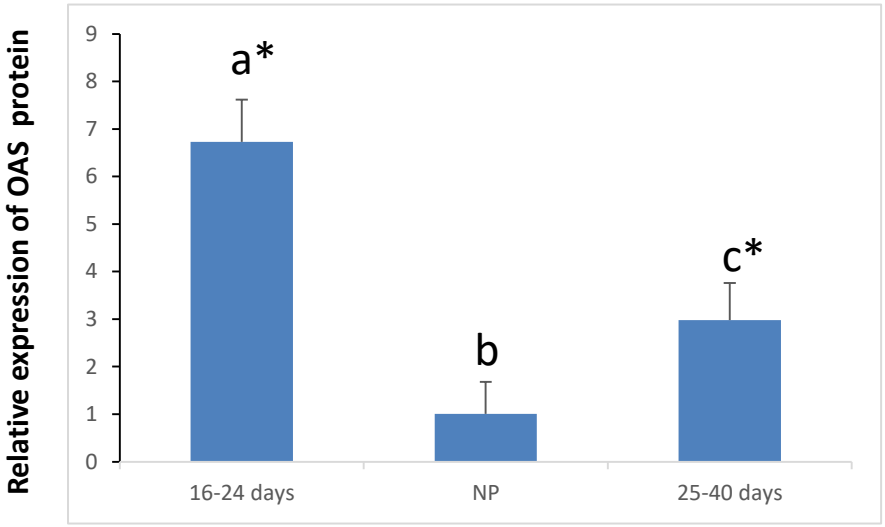

15B

FIGURE 15. Detection of OAS protein by western blotting. Detection of OAS protein on PVDF membrane (A) and relative expression of OAS protein (B) in the endometrial tissue of pregnant and non-pregnant goats. M: Molecular weight markers (Himedia); Lanes 1: Non-pregnant goat; Lanes 2: 16 to 24 days pregnant goat; Lane 3: 25 to 40 days pregnant goats. Bars indicate mean ± SEM values (n = 6). Different alphabets indicate significant difference ($P < 0.05$).